Spring 2022

Regulation of Trio GEF1 Activity by the Spectrin Repeats and Cellular Factors

Josie Evelyn Bircher
Yale University Graduate School of Arts and Sciences, josie.bircher@yale.edu

Abstract

Regulation of Trio GEF1 Activity by the Spectrin Repeats and Cellular Factors

Josie Evelyn Bircher

2022

The Trio family of proteins consists of Trio, Kalirin, UNC-73 (in *Caenorhabditis elegans*) and dTrio (in *Drosophila*). Trio proteins are key regulators of cell morphogenesis and migration, tissue organization, and secretion and protein trafficking in many biological contexts. Recent discoveries have linked Trio and Kalirin to human disease, including neurological disorders and cancer. The genes for Trio family proteins encode a series of large multidomain proteins with up to three catalytic activities and multiple scaffolding and protein-protein interaction domains. As such, Trio family proteins engage a wide array of cell surface receptors, substrates, and interaction partners to coordinate changes in cytoskeletal regulatory and protein trafficking pathways. In Chapter 1, I provide a comprehensive review of the specific mechanisms by which Trio family proteins carry out their functions in cells, highlight the biological and cellular contexts in which they occur, and relate how alterations in these functions contribute to human disease. This sets up the context for a major goal of my thesis, which was to elucidate a regulatory mechanism of Trio catalytic activity and understand how disease associated mutations disrupt this regulation.

In Chapter 2, I describe my co-first author work, which uncovered a mode of Trio regulation. The Trio spectrin repeats (SRs) are adjacent to the Trio GEF1 domain and disease-associated mutations to the SRs have been shown to impact Trio GEF1 activity. I provide evidence that the Trio SRs autoinhibit Trio GEF1 activity via intramolecular interactions, and this is relieved by disease-associated mutations.

In Chapter 3, I discuss unpublished work to understand how Trio is regulated in a cellular context. I cover my work to generate a Trio knockout fibroblast cell line and discover activators of the autoinhibited Trio GEF1 activity. This preliminary work is supported by Chapter 4, in which I describe the most pressing future experiments and approaches I recommend to follow up my thesis work. Together, the work described in this thesis provides insight into a novel mechanism of Trio regulation and sets up a framework for many exciting future discoveries.

Regulation of Trio GEF1 Activity by the Spectrin Repeats and Cellular Factors

A Dissertation

Presented to the Faculty of the Graduate School

Of

Yale University

In Candidacy for the Degree of

Doctor of Philosophy

By

Josie Evelyn Bircher

Dissertation Supervisor: Anthony J. Koleske

May 2022

Table of Contents

List of figures

List of tables

List of abbreviations

ACTH	Adrenocorticotropic hormone
ADAM23	ADAM metallopeptidase domain 23
ADB	Antibody dilution buffer
AJs	Adherens junctions
AP-1	Activator protein-1
ASD	Autism Spectrum Disorder
AU	Arbitrary Units
BME	β-mercaptoethanol
BPD	Bipolar Disorder
BS3	Bis(sulfosuccinimidyl)suberate
Cdk5	Cyclin Dependent Kinase 5
CGNs	Cerebellar granule neurons
CV	Compensation voltage
DCC	Deleted in colorectal cancer
DCV	Dense Core Vesicles
DH	Dbl Homology
DLL4	Delta-like 4
DNA	Deoxyribonucleic acid
Dock180	Dedicator of cytokinesis 180
dTrio	*Drosophila* Trio protein
dTrio	*Drosophila* Trio gene
DTT	1,4-dithiothreitol
EB1	End-binding protein 1
EDTA	Ethylenedianinetetraacetic acid
EGTA	Ethylene glycol-bis(2-aminoethylether)-N N N'N'-tetraacetic acid
EM	Electron microscopy
FA	Focal adhesion
FAIMS	Field asymmetric ion mobility spectrometry
FL	Full-length
fl	*Flox*
Fn	Fibronectin
GDP	Guanosine diphosphate
GDP-FL-BODIPY	GDP-fluorescein-BODIPY
GEF	Guanine nucleotide exchange factor
GFP	Green fluorescent protein
GST	Glutathione-s-transferase
GTP	Guanosine triphosphate
GTPase	Guanosine triphosphate hydrolase
Hr	Hours
HRP	Horseradish peroxidase
ICAM1	Intercellular Adhesion Molecule 1
ID	Intellectual disability

Ig	Immunoglobulin
IP	Immunoprecipitate
IRES	Internal ribosome entry site
Kalirin	Human Kalirin protein
Kalirin	Human Kalirin gene
k_{cat}	Rate constant for conversion of substrate into product
K_D	Dissociation constant
kDa	Kilodalton
K_M	Michaelis constant
KO	Knockout
k_{obs}	Observed rate coefficient
L1CAM	L1 cell adhesion molecule protein
LAR	Protein-tyrosine phosphatase
LC-MS/MS	Liquid chromatography-mass spectrometry
Lgi1	Leucine-rich glioma inactivated 1
MES	2-ethanesulfonic acid
Min	Minutes
mRNA	Messenger ribonucleic acid
MT	Microtubule
N-Cadherin	Neural cadherin
Nav1	Navigator 1
NDDs	Neurodevelopmental disorders
NLGN1	Neuroligin1 gene
NTA	Nitrilotriacetic acid
PAM	Peptidylglycine α-amidating monooxygenase
PCR	Polymerase chain reaction
PH	Pleckstrin homology
PIs	Phosphatidyl inositols
PMSF	Phenylmethylsulfonyl fluoride
Rac1	Ras-related C3 botulinum toxin substrate 1
RFP	Red fluorescent protein
Rho	Ras homology family member
S200	Superdex 200
SAXs	Small angle x-ray scattering
SCZ	Schizophrenia
SDS-PAGE	Sodium dodecyl sulfate – polyacrylamide gel electrophoresis
Sec	Seconds
SEC	Size exclusion chromatography
SH3	Src homology 3
SR	Spectrin repeat
TBS	Tris buffered saline
TCA	Thalamocortical axons
Trio	Human Trio protein
TRIO	Human Trio gene
Unc-73	UNCoordinated 73

Unc-73	*C. elegans* trio protein
unc-73	*C. elegans* trio gene
UPLC	Ultra performance liquid chromatography
VE-cadherin	Vascular endothelial cadherin

Acknowledgements

I first have to thank my advisor, Tony Koleske. Tony has taught me a huge number of things throughout the years, but here are some highlights. Tony taught me how to be a rigorous scientist, think for myself, and be efficient. My graduate school experience was filled with failures. I'm sure this is the norm, but that didn't make it any easier. I could always rely on Tony to be my biggest cheerleader and to say to me "you're doing everything right" when I needed to hear it. This relentless support allowed me to be completely honest in our weekly meetings with whatever I was struggling with, which I think was a huge factor in getting me to the finish line of graduate school. I know he will continue to be my advocate beyond graduation, and I am immensely grateful for that.

I owe an unbelievable amount of thanks to Ellen Corcoran who was my co-author, desk-mate, and friend. I started working on this Trio project relatively late in the game, and she was more than welcoming to have me join her. I learned so much while working closely with her on this project – how to communicate clearly, set boundaries for work and life, and clearly identify goals and deadlines. I think there was a huge learning curve for both of us in this regard, and I am incredibly grateful that I was able to learn how to work together on a project with someone as patient and forgiving as Ellen. I found it incredibly motivating to work on a project with someone else, and highly recommend that people escape the crippling loneliness of graduate school by doing the same.

There were several influential lab mates in the Koleske lab that I worked with during my time here. First, Juliana Shaw and Alex Scherer were instrumental in convincing me to join the lab and teaching me about scientific rigor. Juliana taught me basically everything about doing science, from how to pipette, to not being lazy, and having undying determination. Anytime I had to motivate myself about science, I would say the words 'just try to be as good as Juliana', because I knew that if I ended up half the scientist she was, I would be really great. Alex mentored me through incredible amounts of TIRF strife and taught me how to purify proteins on the FPLC like the structural biologists we both admired. Wanqing Lyu and Kuanlin Wu have provided invaluable advice and energy since I started in the lab. Wanqing is the scientist I currently rely on for advice about anything at all because she has done 10x more experiments than basically anyone else in the lab. Whether I have a stupid question about how to run a DNA gel or want to brainstorm the best experiment, Wanqing is always around and more than willing to talk! I most appreciate Kuanlin for the cheerful energy he brings into lab and the lightheartedness that he approaches science with – it always makes me a little more excited to do science. I also want to acknowledge Xianyun Ye and Elizabeth Velalli for the immense amount of work they do to support the lab; it is not an understatement to say that the lab would fall to pieces without them. I owe hours of my life to Amanda Jeng for the amount of time she has saved me with her impeccably organized notes – any time I needed information about a Trio primer or protocol, she would send it to me in a matter of minutes. Finally, I value the

advice and camaraderie that all other members of the Koleske lab, past and present, not mentioned here, provided to me during my time at Yale.

Throughout my graduate studies, my thesis committee has been a great source of advice and support for me. Thomas Pollard and Mark Solomon each provided unique feedback for my projects. As my thesis project changed pretty drastically throughout the years, they were always supportive and honest about how I was doing. In addition to their scientific input, I always felt they were genuinely interested in how I was doing personally and dealing with the stresses of graduate school. It was great to not feel like I was just expected to be coping perfectly with a stressful situation, especially during the Covid pandemic.

My friends have been incredibly supportive throughout my time in grad school. I was lucky enough to have a core group of supportive friends that were all in grad school together at Yale, as well as a bunch of friends who weren't. It was great to be able to vent people who knew exactly what I was talking about, and also really great to vent to people who had real jobs and lived normal lives with the hope that I would someday be there as well. Briefly, Earnest was always there to tell me it was OK to take a break and not be so hard on myself. Chris and Julia have been my biggest cheerleaders since almost day 1, and were always there to joke or listen about whatever was going on. Frankie is my oldest friend, and despite her life being totally busy, always took extra time to check in and listen to all of my stories. Finally, Carla and Andre took me under their wing at the gym and taught me so much about weightlifting, Ronnie Coleman, and how to generally be a good

friend. I am so lucky to have been surrounded by so many wonderful people throughout my time at Yale.

I'd like to thank my family – my brother Walter, my mom, Mary, and my dad, Craig for always being willing to listen to the struggles I was having in school. Mary and Craig loved to visit New Haven, buy me pizza, and clean my apartment, and it was always great to not have to worry about taking care of myself when they came to visit. It was also an unbelievable privilege to be able to go through grad school at the same time as Walter. Our weekly breakfasts helped me through numerous hard times in grad school and were also wonderful times to talk excitedly about what the future holds.

My work in this thesis was funded in part by F31 NS113511 and T32 GM 7223-44.

Dissertation overview

This dissertation is comprised of 4 parts. In Chapter 1, I review the Trio family of proteins and their impact on cell morphogenesis and motility, with a focus on a known mechanisms of Trio regulation. Most of this chapter was written as a literature review with my advisor, Tony Koleske (1). Chapter 2 covers my co-first author manuscript work which I performed with a fellow graduate student in the lab, Ellen Corcoran (2). In this chapter, we elucidate a novel mode of Trio catalytic activity auto-regulation. Chapter 3 details my unpublished preliminary work to study Trio-based signaling in a cellular context. The work described in Chapters 2 and 3 opens up numerous avenues for future study, so in Chapter 4, I describe the most pressing next experiments as a roadmap for future work to understand regulation of Trio catalytic activity.

Chapter 1

Trio family proteins as regulators of cell migration and morphogenesis in development and disease – mechanisms and cellular context

1.1 Overview

Trio family proteins are key regulators of cell motility and morphogenesis, tissue development, and protein trafficking and secretion in numerous biological contexts, including their prominent roles in developing nervous systems. These diverse roles are achieved through Trio protein interactions with membrane receptors, cytoskeleton-interacting proteins, lipids, endocytic machinery, kinases, and Rho family GTPases in the cell (Fig. 1.1). Recent studies have linked mutations in *Trio* and *Kalirin* to neurological diseases and cancers, highlighting the need to understand the primary functions of Trio family proteins and underscoring the outstanding questions in the field: how are the different catalytic activities balanced within Trio proteins?; how do the accessory domains in Trio proteins contribute to Trio function?; and how does the primary function of Trio proteins differ based on its interactions with cellular binding partners?

Here we review Trio family protein functions from a biochemical level to roles in neurodevelopment and disease. We first discuss the specific catalytic activities of Trio family proteins and how the different domains in Trio family proteins and interactions with signaling partners contribute to Trio family protein catalytic activity and function. We then discuss the specific cellular processes that are driven by these Trio activities. Finally, we address recent studies linking vertebrate Trio to human disease, and how specific disease-associated mutations and rare variants impact Trio function. These sections were originally included in my first-author literature review (1).

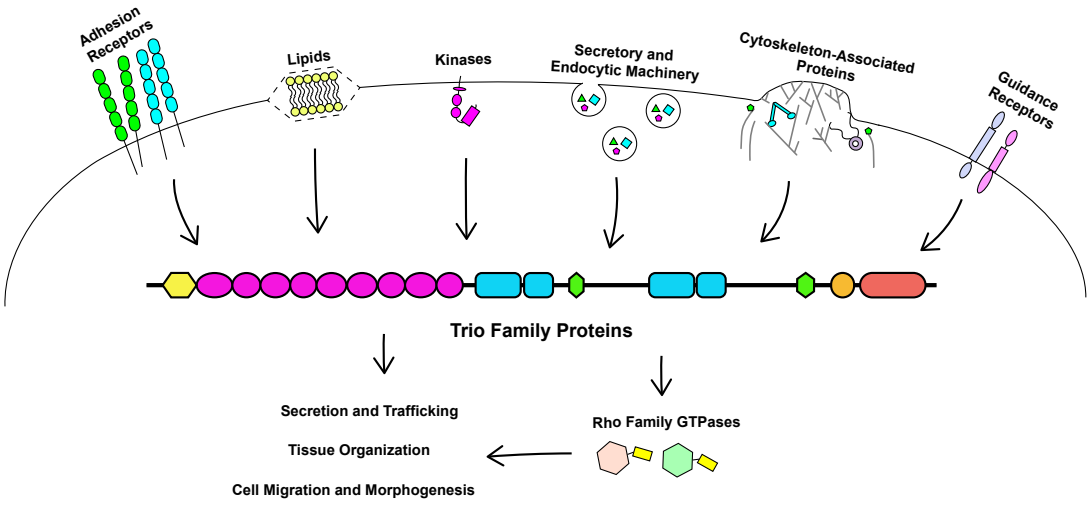

Fig. 1.1 Trio family proteins integrate signaling from a wide array of interaction partners to impact cell behaviors. *Figure adapted from Bircher and Koleske, 2021*

Trio family proteins relay signaling with adhesion receptors, lipids, kinases, secretory and endocytic machinery, cytoskeleton-associated proteins, and guidance receptors to regulate secretion and trafficking, tissue organization, and cell migration and morphogenesis. Much, but not all, of this signaling is achieved through Trio catalytic activities on Rho family GTPases. Domains of the Trio proteins: Yellow – Sec14; Pink – Spectrin Repeats; Blue – Guanine Nucleotide Exchange Factor domains; Green – Src Homology 3 domains; Light orange – Immunoglobulin like domain; Dark orange – Kinase domain.

1.2 The Trio family of proteins

The Trio protein family has four well studied members: two vertebrate paralogs (Trio and Kalirin) and two invertebrate orthologs (UNC-73 in *Caenorhabditis elegans* and dTrio in *Drosophila*). Trio family proteins are large proteins (up to 350kDa), containing up to three catalytic domains, for which they are named; full-length (FL) isoforms of Trio family proteins contain two guanine nucleotide exchange factor (GEF) domains (GEF1 and GEF2), and the vertebrate paralogs contain an additional putative serine/threonine protein kinase domain. Trio family proteins also contain numerous accessory domains that differ slightly across species, and whose functions are poorly understood. Furthermore, alternative splicing produces many different isoforms whose expression profiles vary across tissue and developmental stage (Fig. 1.2).

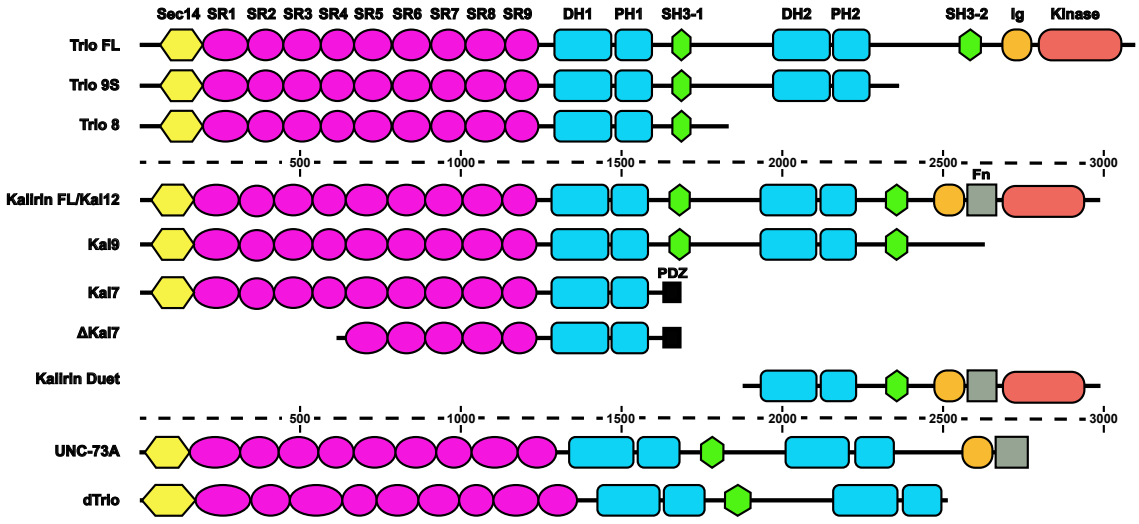

Fig. 1.2: Trio family proteins are large multi-domain proteins that contain up to three catalytic domains and multiple accessory domains. *Figure adapted from Bircher and Koleske, 2021*

All full-length (FL) Trio family proteins (Trio FL, Kalirin FL/Kal12, UNC-73A, and dTrio) contain two catalytic GEF units composed of tandem Dbl homology (DH) and Pleckstrin Homology (PH) domains. The vertebrate members, Trio and Kalirin, also contain an additional putative protein kinase domain. The additional accessory domains vary slightly between species, but include: a Sec14 domain, nine spectrin repeats (SR1-9), one to two Src homology 3 (SH3) domains, and zero to one immunoglobulin-like (Ig) and fibronectin-like (Fn) domains (3-6). Trio, Kalirin, and UNC-73 are alternatively spliced to generate multiple isoforms.

(Figure legend continued on next page.)

Figure 1.2 legend continued: Only the isoforms mentioned in this review are shown here; for a more comprehensive list, see (5,7,8). Amino acid numbers are marked on dotted line for scale.

While Trio and Kalirin have nearly identical domain structures, they have different tissue-specific and temporal expression profiles (9). Trio is ubiquitously expressed, whereas Kalirin is most highly expressed in the nervous system (3,9-11). Additionally, Trio is abundant in the developing brain (12), while Kalirin predominates in the brain from postnatal development through adulthood (13). Finally, different isoforms of Trio vary in abundance in different contexts (7,8). An outstanding question in the field is how small differences between Trio and Kalirin, or the usage of different isoforms, drives Trio family proteins to perform their vast set of distinct tasks within a cell.

1.3 Trio family protein catalytic activities and membrane interactions

Vertebrate Trio family proteins contain two GEF domains and a protein kinase domain, each of which can activate discrete signaling outputs. Several domains within Trio also regulate Trio GEF activities and mediate membrane binding, which brings Trio in proximity to its membrane-bound Rho family GTPase substrates.

Trio family protein GEF domains

The Trio family protein GEF domains catalyze exchange of GDP for GTP on specific Rho family GTPases, master regulators of the cytoskeleton (14). They are comprised of a tandem catalytic Dbl-homology (DH) domain and a regulatory pleckstrin homology (PH) domain, together forming the functional GEF unit. The Trio family GEF1 domain catalyzes GTP exchange on both Rac1 and RhoG *in vitro* (3,5,15-17), although vertebrate Trio GEF1 catalyzes faster exchange on RhoG compared to Rac1 (18-20). In contrast, the Trio family GEF2 domain catalyzes GTP exchange on RhoA *in vitro* (3,5,21), although vertebrate Trio GEF2 does so at a much slower rate than that its GEF1 exchanges GTP on RhoG (22). Vertebrate Trio GEF1 can also catalyze GTP exchange on membrane-anchored Cdc42 (23), suggesting that the GEF1 and GEF2 domains may have additional Rho GTPase targets beyond just Rac1, RhoG, and RhoA.

Loss of endogenous Kalirin or Trio reduces activation of their GTPase targets in cells and tissues, demonstrating that they are major cellular activators of these GTPases (24-27). It is unknown how the Trio GEF1 and GEF2 activities are

balanced in the cell, especially since Rac1/RhoG and RhoA typically have opposing signaling pathways and outputs in cells (28,29). It is also unclear whether the GEF1 domain preferentially targets RhoG over Rac1 in cells; an assessment complicated by the fact that RhoG can activate Rac1 via the Dedicator of cytokinesis protein 1- Engulfment and cell motility protein 1 (Dock180-Elmo) complex during integrin-mediated cell spreading and other processes (30,31). Therefore, whether Trio GEF1 activates Rac1 directly or preferentially through activation of RhoG signaling through Dock180-Elmo is unknown.

GEF activity is modulated by accessory domains and phosphorylation

Accessory domains also modulate the Trio and Kalirin GEF activities. For instance, the PH domain located within each GEF domain impacts catalysis by the adjacent DH domain. The DH1 and PH1 domains of Trio GEF1 coordinately engage Rac1 during GTP exchange, and these direct PH1-Rac1 interactions are critical for efficient exchange (20). The Trio and Kalirin GEF1 domains share 92% sequence identity, so it is likely Kalirin GEF1 shares this regulation mechanism (32). Indeed, removal of the PH1 domain significantly impairs catalytic activity of the purified Trio or UNC-73 GEF1 domains, suggesting this mode of regulation is conserved (17,22,33). In notable contrast, the Trio PH2 makes intramolecular inhibitory contacts with DH2 to block RhoA binding, explaining why loss of Trio PH2 enhances DH2 activity (22,34). Trio and Kalirin only share 67% identity between their GEF2 domains, so it is less clear whether Kalirin GEF2 shares this mode of regulation (32). The Trio and Kalirin SRs also impact GEF1 activity. For example,

Trio SRs 1-5 bind the GEF1 domain directly and inhibit exchange on Rac1 when added in trans to an *in vitro* exchange assay (35). Similarly, Kalirin fragments that contain portions of the SRs plus GEF1 exhibit reduced Rac1 exchange activity relative to purified GEF1 domain alone (36,37). These findings indicate that the PH domains and SRs regulate Trio and Kalirin GEF activities, but they raise questions of how these regulatory interactions are controlled to fine tune these activities in cells.

Trio and Kalirin are phosphorylated by a diverse set of protein kinases (38-46). Phosphorylation events within the GEF domains directly impact GEF activity *in vitro*, indicating phosphorylation as a key mode of regulation (40,44). Phosphorylation of Trio and Kalirin on sites outside the GEF domains also impact active Rac1 levels in cells (45-47), although how these phosphorylation events impact GEF1 activity is less clear. The context and outcome of these events are further discussed below.

Putative protein kinase domain

Several vertebrate Trio and Kalirin splice isoforms contain a putative serine/threonine protein kinase domain that may have protein kinase activity. In support of this, Kalirin Duet is phosphorylated in 3T3 cells, and mutating a predicted key catalytic residue (K2713A) disrupts this event, suggesting autophosphorylation (38). Furthermore, expression of the Kalirin protein kinase domain in cultured rat hippocampal neurons enhances neurite outgrowth, while a predicted catalytically-inactive Kalirin protein kinase mutant blocks neurite

extension (48). These findings strongly suggest that Trio protein kinase activity has physiological roles, but the fundamental questions of how protein kinase activity is regulated and what substrates are targeted remain to be answered.

Membrane localization and regulation of Trio family proteins

Trio proteins contain a lipid-binding N-terminal Sec14 domain and two PH domains, each with the potential to bind phospholipids. Not surprisingly, Trio family proteins localize to diverse membrane regions, including membrane ruffles, cell-cell junctions, and the trans-Golgi network (49-55). Interactions with lipids likely enable Trio proteins to interact with their Rho family GTPase targets, which are themselves targeted to the membrane by covalently attached isoprenoid moieties (56).

The Kalirin Sec14 domain binds to phosphatidylinositols (PIs), including PI 3,4-bisphosphate (PI(3,4)P2), PI3P, and PI4P (37,41,57), which are found in the plasma membrane, endosomes, secretory granules, and the trans-Golgi network. Loss of the Sec14 domain in Kal7 impairs its ability to promote changes in cell shape and dendritic spine length, indicating the importance of lipid interactions for Kal7 function (37,41). In addition, the Trio GEF1 domain binds PIs in the presence of free RhoG, but not Rac1 (19), suggesting that membrane interactions may be impacted in conjunction with substrate recognition by Trio GEF1. Whether Trio or Kalirin PH2 domains also bind to phospholipids has not been directly tested.

Nevertheless, these observations indicate that lipids are critical regulators of Trio and Kalirin function and may even regulate their catalytic activities.

1.4 Trio family proteins in cell migration

Considering their central roles in regulating Rho family GTPases, it is not surprising that Trio family proteins regulate cell migration. Knockdown of Trio in HeLa cells disrupts spreading on fibronectin and impairs chemotaxis towards serum (58). These defects are restored by Trio GEF1 domain expression, but not GEF2 domain expression, indicating that Rac1 and/or RhoG signaling via Trio GEF1 may be the primary driver of this output (58). Similarly, loss of *Kalirin* or chemical inhibition of Kalirin GEF1 in smooth muscle cells significantly reduces serum-evoked cell migration, implicating Kalirin GEF1 activity in this process (11). Since the process of cell migration involves both the extension of the leading edge of a cell (powered by Rac1), and retraction of the trailing edge (powered by RhoA) (59), it is interesting that Trio-driven migration is mainly powered by Trio GEF1 activity. Whether this is due to different intrinsic activities of the Trio family GEF domains, differences in protein localization, or protein:protein interactions is unknown.

Trio family proteins employ <u>both</u> GEF activities to regulate neuronal cell migration. UNC-73 coordinates the migration of neuronal precursor cells during *C. elegans* development. (16,60-64). P cell neuronal precursors do not migrate normally to the ventral midline in *unc-73* mutants, and optimal migration requires both UNC-73 GEF1 and GEF2 activities (16,61,62,64). In addition, brain-specific ablation of *Trio*

in mice with a *nestin-Cre* transgene (*nestin-Trio-/-* mice*)* also disrupts neuronal migration in the cerebellum (25). The activities of RhoA, Rac1, and Cdc42, key coordinators of cell migration, are all reduced in *nestin-Trio-/-* mice (25), providing in vivo evidence that Trio serves as a signal integrator to those three GTPases in the developing brain.

Less is known regarding cell surface receptors or intercellular signaling partners that may regulate Trio GEF activities during cell migration. One interesting candidate is Supervillin4, which links the actin cytoskeleton to the plasma membrane. Trio employs its 6^{th} and 7^{th} SRs to bind Supervillin4 directly (65). Supervillin4 expression in HeLa cells induces Rac1 activation, and depletion of Trio prevents this, suggesting Supervillin4 signals through Trio to activate Rac1. Furthermore, loss of Trio, Supervillin4, or expression of dominant-negative Trio that interacts with Supervillin4 but cannot activate Rac1, inhibits initial cell spreading, implicating Supervillin4-Trio-Rac1 signaling in cell spreading (65).

1.5 Trio family proteins in cell morphogenesis

Trio family proteins employ their GEF activities downstream of cell surface receptors to regulate cell morphogenesis. The ability of Trio proteins to regulate these processes also depends on a collection of interaction partners and substrates in different cell types. Here we discuss the interaction partners and mechanisms by which Trio regulates changes in cell shape in different cell types.

Cytoskeletal reorganization and cell-edge protrusions

Trio family proteins employ their noncatalytic domains to engage actin- and microtubule (MT)- binding proteins, including Supervillin4, CARMIL, Tara, Filamin, EB1, and Nav1; this impacts their regulation of their target GTPases, thereby modulating cell morphology and behavior (35,58,63,65-67). It remains unknown whether Trio family proteins bind actin or MTs directly.

Overexpression of Trio-FL or the GEF1 domain alone decreases stress fiber formation in fibroblast cells and increases cortical actin filament numbers in HeLa cells (58,68). These phenotypes match those obtained by expression of constitutively active Rac1 and RhoG, consistent with a role for GEF1 activity in driving these changes (69-71). In contrast, Trio GEF2 domain expression increases stress fiber abundance in cells, which phenocopies the constitutive RhoA activation (58,68,72). It is unclear how the opposing outputs of the Trio GEF1 and GEF2 domains are balanced in the context of Trio-FL. However, GEF1 activity appears to dominate, since the phenotypes resulting from Trio-FL expression most closely those following expression of the GEF1 domain alone.

Trio family proteins also promote cell-edge protrusions in various cell types. The Trio and Kalirin GEF1 domains induce cell edge ruffling, protrusions, and/or lamellipodia formation, which are mediated by Rac1 or RhoG, depending on cell type and context (5,18,49,58,68,72,73). For instance, Trio or Kalirin GEF1 expression induces normally spindle-shaped AtT20 cells to adopt a flattened, round morphology, with uniform radial lamellipodia (Ferraro et al., 2007),

characteristics also observed in AtT20 cells with constitutively active RhoG or Rac1 (70). In addition, UNC-73 GEF1 activity, which acts on ced-10 (Rac1) or mig-2 (RhoG), promotes epithelial cell edge protrusions during intercalation of epidermal cells (63,74,75). Finally, co-expression of a dominant-negative RhoG (F37A) with Trio GEF1 in fibroblasts eliminates Trio-induced lamellipodia (18), whereas Rac1 knockdown reduces the ability of Trio GEF1 to induce membrane ruffles in HeLa cells (58). Hence, while Trio family protein GEF1 domains clearly promote cell edge protrusions, whether this occurs via distinct Rac1 or RhoG signaling, or by integrating activation of both, is unclear. Roles for the full-length Trio family proteins or the GEF2 domains in cell edge protrusion have not been extensively characterized.

Axon pathfinding

Significant changes in cell morphology occur in neurons as they elaborate axonal and dendritic processes to form connections with other neurons. Trio family proteins have widespread roles in regulating axon pathfinding. In the fly central nervous system, loss of dTrio function results in mistargeting of individual axons both in central and peripheral neurons (6,42,76,77). Similarly, thalamocortical axons (TCAs) in *Trio-/-* mice stall and misroute in the ventral telencephalon and, ultimately, do not reach their cortical targets (26).

Both Trio family GEF1 and GEF2 activities mediate axon pathfinding processes that are often opposing, suggesting that specific Trio activities can be utilized depending on the needs of the cell. Trio acts downstream of the Deleted in

Colorectal Cancer (DCC) family of guidance receptors to mediate attractive growth of axons toward sources of the secreted guidance cue netrin (Fig. 1.3) (42,45,76,78,79). Deletion of *Trio* eliminates Rac1 activation by netrin in mouse cortical explants and blocks netrin-induced axon outgrowth in cortical, spinal cord, and cerebellar explants (25,78). Likewise, expression of DCC in neuroblastoma cells induces neurite outgrowth, but this is blocked by co-expression of a Trio9 mutant lacking GEF1 activity (78). Treatment of rat cortical explants with netrin also induces Trio phosphorylation at Y2622 by Fyn (45). Accordingly, loss of Trio in rat cortical axons causes axon outgrowth defects that cannot be rescued with a nonphosphorylatable Y2622F Trio mutant, suggesting that Trio phosphorylation is important for netrin signaling (45). Additionally, loss of Trio reduces surface levels of DCC, indicating interactions with Trio may be critical for proper receptor localization (45). It is not understood whether or how Trio binds DCC directly. Trio family proteins also mediate signaling by the Robo/Sax3 family of receptors for repellent Slit ligands in *C. elegans* and vertebrates (Fig. 1.3) (26,80,81). Slit2 induces growth cone collapse in cultured neurons and this response is not observed in *Trio-/-* axons (26). Application of recombinant Slit2 to mouse fibroblasts activates RhoA, but this response is absent in *Trio-/-* mouse embryo fibroblasts, confirming a requirement for Trio GEF2 in mediating Slit2 signaling (26). A major unresolved question is how the netrin/DCC and Robo receptors engage Trio differently to engage GEF1-mediated attractant responses or GEF2-mediated repellent responses, respectively.

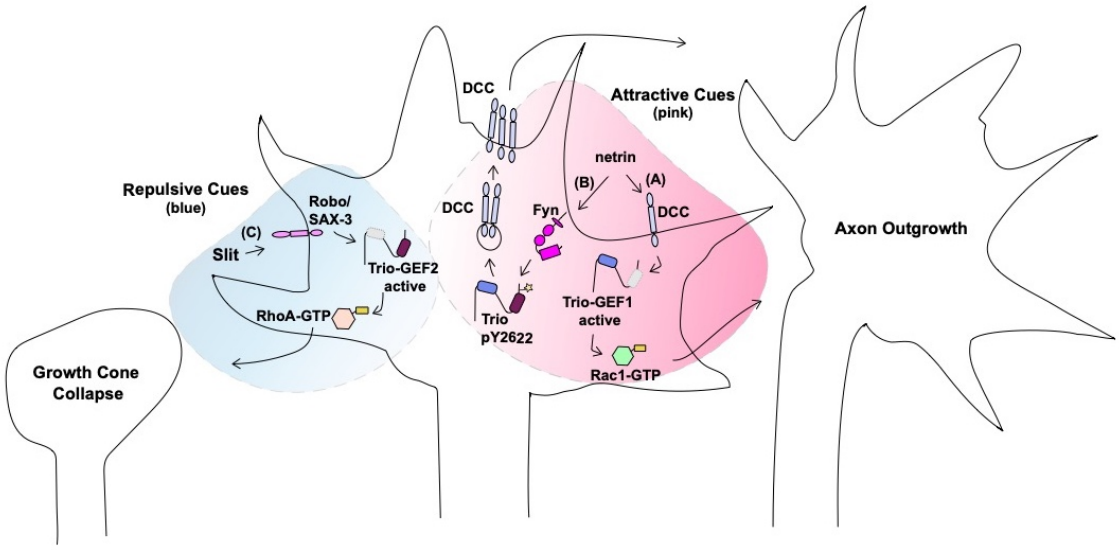

Fig. 1.3 Trio family proteins respond to axon guidance cues through guidance receptors. *Figure adapted from Bircher and Koleske, 2021*

Trio family proteins respond to both attractive and repulsive guidance cues, which induces either axon outgrowth or growth cone collapse. (A) In the presence of netrin, the netrin receptor/Deleted in Colorectal Cancer (DCC) interacts with Trio - it is unknown if this interaction is direct. This interaction results in a Trio GEF1-mediated activation of Rac1, which is necessary for axon outgrowth (78). (B) Netrin stimulation also induces phosphorylation of Trio at Y2622 by Fyn protein Kinase, which leads to increased surface levels of DCC (45). While the roles of Trio in pathways (A) and (B) have not been explicitly connected, Trio-dependent stimulation of DCC at the surface (B) likely constitutes a positive feedback loop to amplify more netrin:DCC signaling in (A). (Figure legend continued on next page)

(Figure legend 1.3 continued) (C) In contrast, Slit binding to the Robo/SAX-3 receptors results in Trio GEF2-mediated RhoA activation, which causes growth cone collapse (26).

Dendritic arbor formation and spine structure

Developing neurons form elaborate branched dendritic arbors studded with small protrusions called dendritic spines that serve as the receptive antennae for synaptic input. Disruption of *Kalirin* or *Trio* leads to significant reduction of dendritic arbor development in mouse cortical layer 5 pyramidal neurons (48,82). Reduced dendritic arbors are also observed in cultured neurons following knockdown or knockout of *Kalirin* or *Trio* (48,82,83), demonstrating that both proteins act cell autonomously to control dendritic arbor development. Chemical inhibitors of Trio GEF1 activity reduce dendritic arbor development, suggesting a downstream requirement for activation of Rac1 or RhoG (48). Trio also regulates neurite morphology, using its SRs to impact Golgi-derived vesicle trafficking, discussed further below (52). Thus, Trio and Kalirin act via multiple catalytic and scaffolding roles to regulate dendritic arbor structure.

While ablation of Trio from cortical excitatory neurons yields smaller dendritic arbors, the remaining dendrites have higher densities of dendritic spines. However, dendritic spines on *Trio-/-* cortical neurons in vivo are also smaller and thinner, having a more immature appearance (82). Interestingly, overexpression of Kal7, the predominant Kalirin isoform in the postnatal brain, is sufficient to drive dendritic spine formation in a manner that depends on its GEF1 activity (84). Kal7 is even capable of inducing dendritic spine like protrusions in inhibitory neurons, which normally lack them (84).

Adhesion at the synapse

The postsynaptic proteins EphB2 tyrosine protein kinase and Neuroligin-1 engage their presynaptic partners EphrinB and Neurexin, respectively, to mediate synapse formation in a manner that also depends on Trio family proteins. First, EphB2 phosphorylates Kal7 and recruits it to synaptic clusters in dendritic spines, and Ephrin signaling through Rac1 is dependent on Kalirin GEF1 activity in primary cultured hippocampal neurons (21,85). Secondly, overexpression of Neuroligin-1 in hippocampal organotypic slices increases dendritic spine density and functional synapses, which also requires Kalirin (86). Finally, *unc-73* regulates extension of muscle arms (87), the postsynaptic contact at the *C. elegans* neuromuscular junction. Collectively, these findings demonstrate that Trio family proteins play evolutionarily conserved functions in regulating post-synaptic development.

1.6 Vertebrate Trio in tissue organization

Vertebrate Trio regulates tissue organization by mediating signaling from transmembrane adhesion receptors including cadherins and Notch1 (Fig. 1.4) (88-90). Cadherins mediate cell-cell adhesions that are crucial for maintaining blood vessel wall integrity (91). Vascular endothelial (VE)-cadherins mediate homotypic interactions, or adherens junctions (AJs), between endothelial cells that comprise the vessel wall and provide a barrier to permeability (91). Two important processes regulate barrier permeability: (1) laminar flow and (2) heterotypic interactions with other non-endothelial cells (90-92). Through various signaling mechanisms, these distinct inputs reinforce existing adhesion sites and induce Rac1 activation to

recruit VE-cadherins to nascent adhesion sites (88). In the absence of flow or heterotypic cell interactions, endothelial cells lacking Trio make unstable and irregular AJs.(88) Recovery of these deficits requires Trio GEF1 catalytic activity and Rac1 activity, suggesting that Trio directly activates Rac1 in regulating VE-cadherin based AJs (88). Importantly, Trio utilizes SRs 5 and 6 to bind the VE-cadherin intracellular tail and co-localizes at AJs with VE-cadherin and sites of focally increased Rac1 activity (88). While these data suggest that VE-cadherin recruits Trio to AJs to induce local activation of Rac1 and reinforce AJs at cell-cell junctions with no stimulus, Trio also plays a role in strengthening AJs in response to laminar flow and heterotypic interactions.

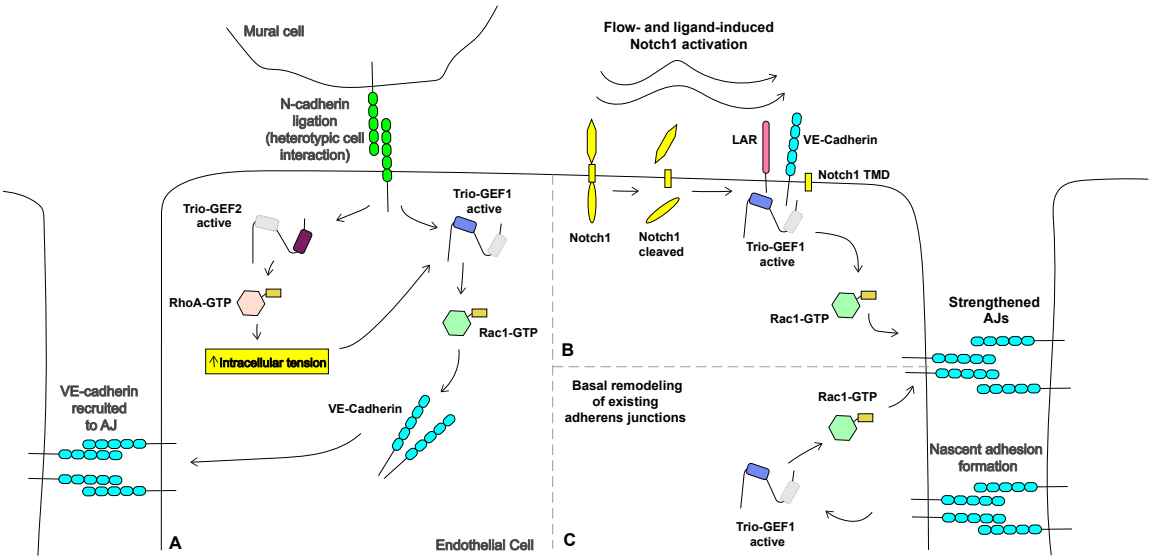

Fig. 1.4 Trio family proteins utilize both GEF domains to promote endothelial adherens junctions. *Figure adapted from Bircher and Koleske, 2021*

Trio family proteins are important for maintaining adherens junction (AJ) integrity between endothelial cells. AJ formation and integrity are impacted by interactions with other types of cells (mural cells), laminar flow, and the basal remodeling of AJs. (A) Neural (N)-cadherin ligation between a mural cell and an epithelial cell induces Trio GEF1 to activate Rac1, increasing vascular endothelial (VE)-cadherin recruitment to AJs between neighboring endothelial cells (90). How N-cadherin signals to Trio, and how Rac1 activation increases VE-cadherin recruitment to AJs in this context, are unknown. N-cadherin ligation also increases Trio GEF2-mediated RhoA activation, increasing intracellular tension, and serving as a positive feedback (Figure legend continued on next page)

(Figure legend 1.4 continued) loop to reinforce the activity of Trio GEF1 (90). It is unclear how N-cadherin signals to Trio GEF2 and how intracellular tension influences Trio GEF1 activity. (B) Notch1 is cleaved upon interaction with ligand Delta-Like 4 (DLL4) under conditions of laminar flow, which allows the Notch1 transmembrane domain (TMD) to colocalize with protein-tyrosine phosphatase (LAR), VE-Cadherin, and Trio. By an unknown mechanism, assembly of this Notch1:LAR:VE-Cadherin:Trio complex induces Trio GEF1 activation of Rac1, which strengthens AJs (89). (C) In basal conditions, AJs are constantly remodeled (91). Ligation of VE-cadherins in the formation of new AJs recruits Trio GEF1 to nascent AJs and subsequent local Trio GEF1-mediated Rac1 activation to strengthen nascent adhesions (88). Trio binds directly to VE-cadherin so this interaction likely drives Trio recruitment to AJs (88).

Notch1 is a single-pass transmembrane protein essential for maintaining AJ integrity. In response to laminar flow, Notch1 is activated in a process that also depends on its extracellular interaction with ligand Delta-Like 4 (DLL4) (89,92). This activation is followed by the initial cleavage of the extracellular domain by metalloproteases and subsequent cleavage of the intracellular domain by the γ-secretase complex (89,92). The remaining transmembrane domain can then form a complex with protein-tyrosine phosphatase (LAR), VE-cadherin, and Trio (89). Formation of this complex is associated with increased Rac1 activity and strengthened VE-cadherin based AJs (89). While Trio, LAR, and Notch1 are required for this process, it is unclear if Trio GEF1 activity is directly responsible for the Rac1 activation that increases barrier strength in this context.

Neural (N)-cadherins mediate heterotypic interactions between endothelial cells and vascular smooth muscle cells or pericytes, collectively called mural cells. These interactions ultimately increase the formation of AJs between endothelial cells (90). When a mural cell adheres to an endothelial cell via N-cadherin, Trio GEF1 becomes activated as measured by its increased binding to nucleotide-free Rac1 and RhoA (90). This increase in activity promotes VE-cadherin recruitment to AJs, thereby strengthening barrier function (90).

Trio is also implicated in the process of transendothelial migration (93,94), where bloodstream leukocytes migrate between endothelial cells to enter tissues, and in the formation of muscular tissue (95). Overall, Trio has a hand in multiple adhesion pathways and plays a clear role in regulating tissue formation, often utilizing its

GEF1 activity to do so. The impact of other Trio protein family members on tissue organization is less well understood.

1.7 Trio family proteins in secretion and intracellular trafficking.

Kalirin was first identified through its association with the neuropeptide processing enzyme peptidylglycine α-amidating monooxygenase (PAM), which is secreted along with neuropeptides in dense core vesicles (DCVs) (10). Subsequent work has shown that Trio family proteins play widespread roles in regulating the secretion and trafficking of membrane-bound vesicles, which we review here.

Secretion and endocytosis

Trio and Kalirin control both secretion and endocytosis in cells. Trio and Kalirin both interact with PAM through their SRs, and co-expression of PAM with Kalirin in AtT20 cells, adrenocorticotropic (ACTH)-secreting pituitary tumor cells, increases ACTH secretion (96). Overexpression of the Trio or Kalirin GEF1 domain alone in AtT20 cells stimulates secretion, and this requires GEF1 catalytic activity (70), although exactly how GEF1 activity promotes secretion is unknown. Cyclin dependent kinase 5 (Cdk5) appears to be a key regulator of Trio in controlling secretion. The Cdk5 inhibitor roscovitine reduces active Rac1 levels in HEK293 cells that express both Trio FL and PAM, and significantly reduces stimulated secretion of ACTH, prolactin, and growth hormone from cultured rat anterior pituitary cells (47). Kalirin and Trio are both phosphorylated by Cdk5 *in vitro* (44,47), suggesting that Cdk5 phosphorylates Trio to increase Rac1 activation and

regulate secretion, although the key regulatory sites and mechanism of this regulation are not known.

Trio family proteins also regulate synaptic vesicle release in neurons. Glutamate release at excitatory synapses is deficient in *Trio-/-* neurons in vivo (82). In *C. elegans*, loss of *unc-73* reduces the release of peptide neurotransmitters via DCVs (97), and genetic manipulation and rescue experiments indicate that signaling from UNC-73 GEF2 is necessary and sufficient to mediate DCV release and support normal locomotion in this context (97). It is not clear if the vertebrate Trio family members regulate DCV release via a similar GEF2-dependent mechanism. These data suggest that Trio family proteins may act through multiple outputs to coordinate vesicle release. Interestingly, Trio and Kalirin also regulate postsynaptic responses (46,82,98), and several studies have implicated Trio and Kalirin in endocytosis (37,99), indicating possible key functions for Trio family proteins on both sides of the synapse.

Intracellular vesicle trafficking

Trio regulates intracellular vesicle trafficking in cerebellar granule neurons (CGNs). Trio colocalizes with Golgi markers and uses its SRs to interact with Rabin8, an activator of the Rab8 and Rab10 GTPases, which are key regulators of Golgi-derived vesicle trafficking (52). Loss of Trio in CGNs significantly impairs Rabin8 activity and Golgi-derived vesicle trafficking. Since trafficking of membrane-embedded cargo from Golgi outposts is essential for dendritic arbor development and maintenance (100), it is no surprise that this impaired vesicle trafficking also

correlates with deficits in neurite extension and reduced neurite length in *Trio-/-* CGNs (52). Indeed, a constitutively active Rab8 mutant rescues these neurite extension defects in *Trio-/-* CGNs (52). This provides an interesting connection between the role of Trio in vesicle trafficking and regulating cell morphology. Overall, it is still unclear whether the interactions between the Trio SRs and Rabin8 are sufficient for regulating trafficking, or if other Trio catalytic activities are required as well.

1.8 Disease-associated mutations and rare Trio variants

Disrupted Trio and Kalirin function have been connected to human disease, including neurological disorders, cancer, and vascular disease. While Trio and Kalirin display high sequence similarity, their disease associations differ. *Trio* has been widely studied for its disease relevance in cancer and neurodevelopmental disorders (NDDs). In contrast, Kalirin has been implicated in a few instances with neurodevelopmental disorders, but also neurodegenerative disorders and vascular disease. Interestingly, recent whole exome sequencing studies have identified Trio, but not Kalirin, as having mutations associated with autism spectrum disorder (ASD) (101) and schizophrenia (SCZ) (102). Since Trio is more highly expressed during development than Kalirin (7,12), it is unsurprising that disruptions to Trio, but not Kalirin, would be associated with neurodevelopmental disorders. However, the molecular mechanisms driving these changes remain poorly understood.

Changes in expression level or genetic variants in Kalirin have been associated with SCZ, Alzheimer's disease (AD), and vascular disease. mRNA levels of *Kalrn* are significantly decreased in the dorsolateral prefrontal cortex of SCZ patients (103). Re-sequencing analyses also revealed a significant association between a Kalirin P2255T mutation and SCZ, though the specific effect of this mutation is unknown (104). Kalirin has also been connected to AD pathology, as there are decreased levels of mRNA in the hippocampus of patients with AD (105). Finally, single-nucleotide polymorphisms in Kalirin are associated with risk of ischemic stroke and early-onset coronary artery disease, but the specific effects of the polymorphisms are unknown (106-109).

Increases in *Trio* gene expression and protein levels occur in numerous cancers. The *Trio* gene resides in a chromosomal region that is commonly amplified in cancer, increasing its gene copy number. *Trio* mRNA levels are increased in carcinomas of the bladder, breast, liver, oral cavity, and cervix, in soft tissue sarcomas, and in glioblastoma (110-119). Higher Trio expression correlates with poor prognosis in individuals with glioblastoma, breast cancer, and hepatocellular carcinomas (112,115,116).

Elevation of Trio levels or signaling is associated with cancer progression. High Trio pY2681 levels correlate with poor prognosis in patients with colorectal cancer after surgery, supporting the idea that increased Trio-mediated signaling promotes cancer progression (40). Trio promotes cell proliferation by integrating signals from Gαq to the transcription factor Activator Protein (AP)-1 and promoting DNA

synthesis (119). Indeed, loss of Trio impairs the ability of HeLa cell tumors to grow in vivo (119). Finally, depletion of Trio in multiple cancer cell lines also reduces invasive cell migration (115,117). Thus, Trio likely plays a role in several aspects of cancer progression, from invasive cell migration to cell proliferation.

De novo mutations and ultrarare damaging variants in *Trio* are also associated with NDDs (101,102,120-122). Many of these *Trio* variants are heterozygous nonsense mutations that reduce Trio protein levels or missense mutations that disrupt Trio function (101,102,120,121). Behavioral and anatomical phenotypes related to loss of Trio protein, which mimics the nonsense mutations, have been thoroughly described (82). Interestingly, many of the *Trio* missense mutations associated with these disorders cluster in specific regions of the gene, and many directly impact Trio catalytic function (Fig. 1.5).

Mutations in the *Trio* GEF1 or adjacent regions are associated with intellectual disability (ID), autism spectrum disorder (ASD), developmental delay (DD), SCZ, and microcephaly (101,120-122). Many of these mutations disrupt highly conserved residues at the Rac1-Trio DH1 binding interface that impact GEF1 exchange activity (101,120-122). Interestingly, some mutations increase GEF1 activity, while others impair it (101,120,121). For instance, the Trio K1431M mutation found in ASD increases GEF1 activity 8-fold (101,120) and disrupts the ability of Trio to support normal synapse development (101). Other variants in the GEF1 domain, like the mild ID- and microcephaly-associated E1299K, R1428Q, and H1469K, compromise GEF1 activity (121). One variant associated with ID,

D1368V, which lies in the DH1 domain but outside the Rac1-DH1 interface, instead hyperactivates Rac1 in HEK293 cells (101). Thus, functional studies of these mutations suggest that both increased and decreased Rho GTPase signaling mediated by Trio contributes to the pathology of NDDs.

Mutations in other *Trio* domains, including the SRs and GEF2 domains, are also associated with NDDs. A cluster of mutations in SR8, including T1075I and R1078W/G/Q, are associated with distinct phenotypes in individuals with DD and macrocephaly (121). These mutations increase Trio GEF1-dependent activation of Rac1 (121), but it is not known how this gain of function allele contributes to macrocephaly. We elucidate the mechanism of the spectrin repeat mutation impact on GEF1 activity in Chapter 2. Finally, a single *de novo* mutation in the GEF2 domain, associated with bipolar disorder (M2145T), increases GEF2 exchange activity four-fold, highlighting the importance of both GEF activities of the Trio protein (120). Taken together, these findings are clear examples that alterations in Trio catalytic activities lead to distinct NDD phenotypes.

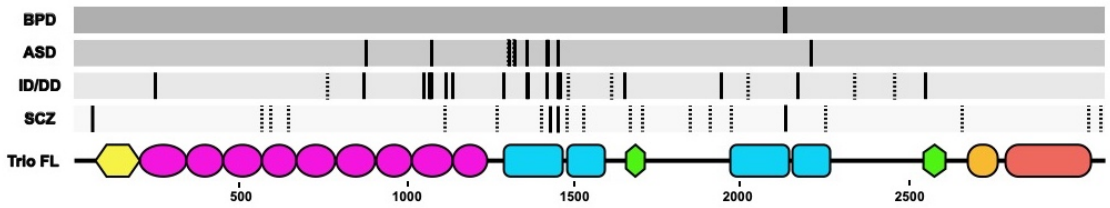

Fig. 1.5 Trio family protein mutations. Figure adapted from Bircher and Koleske, 2021

Specific locations of Trio mutations associated with various neurodevelopmental disorders. Interestingly, mutations to Trio cluster in distinct regions of the gene, many clustering around the first GEF domain. Solid lines indicate missense mutations; dotted lines indicate nonsense mutations. BPD – Bipolar Disorder; ASD – Autism Spectrum Disorder; ID – Intellectual Disability; DD – Developmental Delay; SCZ – Schizophrenia. Domains of Trio: Yellow – Sec14; Pink – Spectrin Repeats; Blue – Guanine Nucleotide Exchange Factor domains; Green – Src Homology 3 domains; Light orange – Immunoglobulin like domain; Dark orange – protein Kinase domain.

1.9 Remaining questions and future challenges

Genetic, biochemical and cell-based studies of Trio family proteins have revealed many important functions for these proteins, cellular contexts in which they act, and their key roles in human disease. However, many questions remain. Some of the biggest unresolved questions center on the catalytic functions of Trio. Why do many Trio isoforms contain two distinct GEF domains, especially when they act on distinct substrates that often have opposing cellular roles? Are the distinct GEF activities coordinated in cells and, if so, how? How do the accessory domains in Trio alter GEF activity, through phosphorylation, interactions with cellular binding partners, or autoregulation? Finally, does the Trio protein kinase domain have substrates and significant signaling outputs in cells? While some of these questions are addressable with current biochemical approaches, some will require advances in single-molecule enzyme assays and/or single molecule live cell imaging. Addressing these questions will reveal how distinct cell receptors and intracellular binding partners differentially impact Trio catalytic activities and help unveil the possible distinct functions of the various isoforms of each gene. With the exception of individual domains, the structures of the entire Trio proteins are largely unknown, in particular with regard to how their domains are arranged in three dimensions, the extent to which domain-domain interactions are regulated and how they are impacted by interactions with other cellular partners. Advances in electron cryo-microscopy and electron cryo-tomography should facilitate the three-dimensional reconstructions of specific Trio proteins and enable the field to study their structure and interactions in their native cellular context.

Overall, Trio family proteins play incredibly diverse roles in cells, and their disruptions are associated with cancer progression and neurodevelopmental disorders. The ubiquitous roles of these proteins in biological systems highlights the need to fully understand their exact function, and why disruption of their functions impacts development and yields disease.

Chapter 2

Regulation of Trio GEF1 by the spectrin repeats

2.1 Overview

De novo mutations and ultra-rare variants in *TRIO* are enriched in neurodevelopmental disorders (NDDs) (1,101,120,122,123) and the pattern of these variants differs in different disorders. For example, de novo missense and rare damaging variants in the GEF1 domain and adjacent regulatory SRs are enriched in autism, intellectual disability, and developmental delay, suggesting that dysregulated GEF1 activity contributes to the pathophysiology of these disorders. Indeed, our lab and others have shown that some of these variants disrupt the ability of GEF1 to catalyze Rac1 activation (101,120-122). However, the role of the SRs in Trio function and the impact of disease-associated variants remains unknown.

Previous studies demonstrated that expression of Trio GEF1 increased Rac1 activity in cells, and resulted in dominant gain-of-function pathfinding defects in fly retinal axons (77,124). Appending additional regions of Trio, including the SRs, to GEF1 attenuated both Trio GEF1-dependent processes. These observations strongly suggest that the SRs reduce GEF1 activity in Trio. However, it remains unknown whether the SRs autoinhibit GEF1 activity directly or via the recruitment of cellular cofactor(s). It is also unclear how variants in the SRs would impact this regulatory mechanism in vitro and in cells.

We provide evidence here that SRs 6-9 directly inhibit Trio GEF1 activity in vitro and in cells. Using a GDP-FL-BODIPY nucleotide exchange assay (125), we show

that inclusion of SRs 6-9 is sufficient to inhibit GEF1 activity in vitro, suggesting an autoinhibitory mechanism, and that NDD-associated variants in the SR8 and GEF1 domains increase GEF1 activity by relieving autoinhibition. Using chemical cross-linking and BioLayer Interferometry, we demonstrate that the SRs make contact with the pleckstrin homology (PH) region of the GEF1 domain and reduce the affinity of GEF1 for Rac1. Together, our findings provide a novel RhoGEF regulatory mechanism by which SRs disrupt Trio GEF activation by reducing interaction of Trio GEF with Rac1 and impairing catalytic efficiency. This mechanism appears to be commonly disrupted in NDDs, making it a potential target for therapeutic intervention.

This work is my first author work in collaboration with my co-author, Ellen Corcoran. It was submitted to JBC in 2022 (2), and the following sections are taken directly from the submitted work.

2.2 Results

Inclusion of SRs 6-9 reduces Trio GEF1 activity.

Genetic variants in SRs 6-9 are associated with NDDs, some of which were previously shown to affect Trio-mediated Rac1 activation in cells. To measure the impact of the SRs on GEF1 activity in vitro, we generated and purified Trio GEF1 alone (42 kDa) or a Trio fragment containing SRs 6-9 appended to the GEF1 domain (SR6-GEF1, 99 kDa) (Fig. 2.1*A*). Both proteins were monodisperse upon

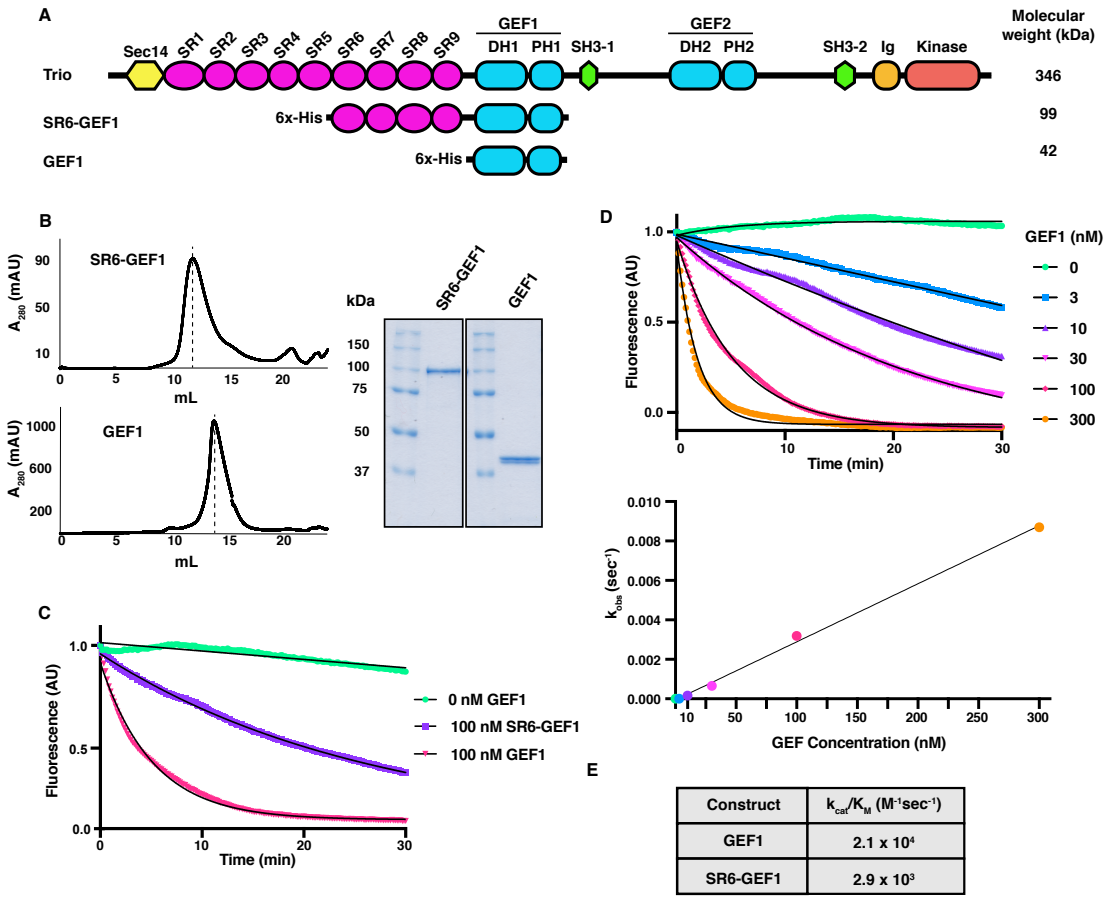

Fig. 2.1 Inclusion of SRs 6-9 reduces Trio GEF1 activity on Rac1. *Figure adapted from Bircher, Corcoran et al., 2022*

(A) Schematic of Trio proteins: Full-length Trio, SR6-GEF1, and GEF1. SR-spectrin repeat; DH1-Dbl homology domain; PH1-pleckstrin homology domain; SH3-1 – Src homology 3 domain. Ig Ig-like domains. (B) Trio SR6-GEF1 and GEF1 were purified and size exclusion chromatography was performed to verify that proteins were monodisperse. Dotted lines indicate peak elution volume used to calculate Stokes radii. Samples (approximately 5 µg) of purified components were

(Figure legend continued on next page)

(Figure legend 2.1 continued) analyzed by SDS-PAGE and stained with Coomassie Blue to assess purity. (C) 100 nM of Trio GEF proteins were incubated with 12.8 μM Rac1 preloaded with 3.2 μM BODIPY-FL-GDP (concentrations optimized for best signal:noise ratio), and nucleotide exchange was tracked via the decrease in fluorescence over time. Trio SR6-GEF1 had approximately 10-fold lower exchange activity compared to GEF1 alone. Representative trace shown here, n=22 for overall quantification of rates. Traces in color, exponential fits overlaid in black. (D) GEF1 catalytic efficiency was determined by measuring the k_{obs} of GEF1 at multiple concentrations. Sample traces shown with exponential fits overlaid in black. This analysis was performed for both GEF1 and SR6-GEF1 two times for quantification. (E) The catalytic efficiency of SR6-GEF1 was nearly 90% lower than GEF1 (n=2). Values are reported as an average of two independent replicates.

size exclusion chromatography and eluted at a position consistent with being monomers (estimated Stokes radius was 3.8 nm for GEF1, 5.6 nm for SR6-GEF1) (Fig. 2.1*B*). Using a fluorescence-based guanine nucleotide exchange assay, we measured the catalytic activity of GEF1 and SR6-GEF1. Purified 100 nM GEF1 efficiently catalyzed exchange of BODIPY-FL-GDP for GTP on Rac1, with a first-order dissociation rate constant k_{obs} = 2.9 ± 1.1 x10^{-3} s^{-1} (Fig. 2.1*C*). Measurement of the rate constant k_{obs} as a function of GEF1 concentration yielded a k_{cat}/K_M = 2.1 x 10^4 M^{-1} s^{-1} (Fig. 2.1*, D* and *E*). SR6-GEF1 similarly promoted GTP exchange onto Rac1, but with a significantly reduced (~95% and 90%, respectively) k_{obs} = 1.6 ± 2.4 x10^{-4} s^{-1}, and k_{cat}/K_M = 2.9 x 10^3 M^{-1} s^{-1} (Fig. 1,*C* and *E*). These observations indicate that inclusion of SRs 6-9 autoinhibits Trio GEF1 activity on Rac1 in vitro.

NDD-associated variants in SR8 increase Trio GEF1 activity in the context of SR6-GEF1.

We generated and purified SR6-GEF1 expression constructs containing single NDD-associated variants in either SR6 or SR8 and measured their ability to catalyze nucleotide exchange on Rac1 (Fig. 2.2, *A* and *B*). When tested at 100 nM, all SR8 variants, except N1080I, increased the k_{obs} by 3-7-fold over that of WT SR6-GEF1 (Fig. 2.2, *C* and *D*). In agreement with these findings, one representative SR8 variant, SR6-GEF1$_{R1078Q}$, which had a significantly increased k_{obs} = 1.4 ± 0.5 x10^{-3} s^{-1}, had a k_{cat}/K_M = 4.4 x 10^3 M^{-1} s^{-1}, a 1.5-fold increase in

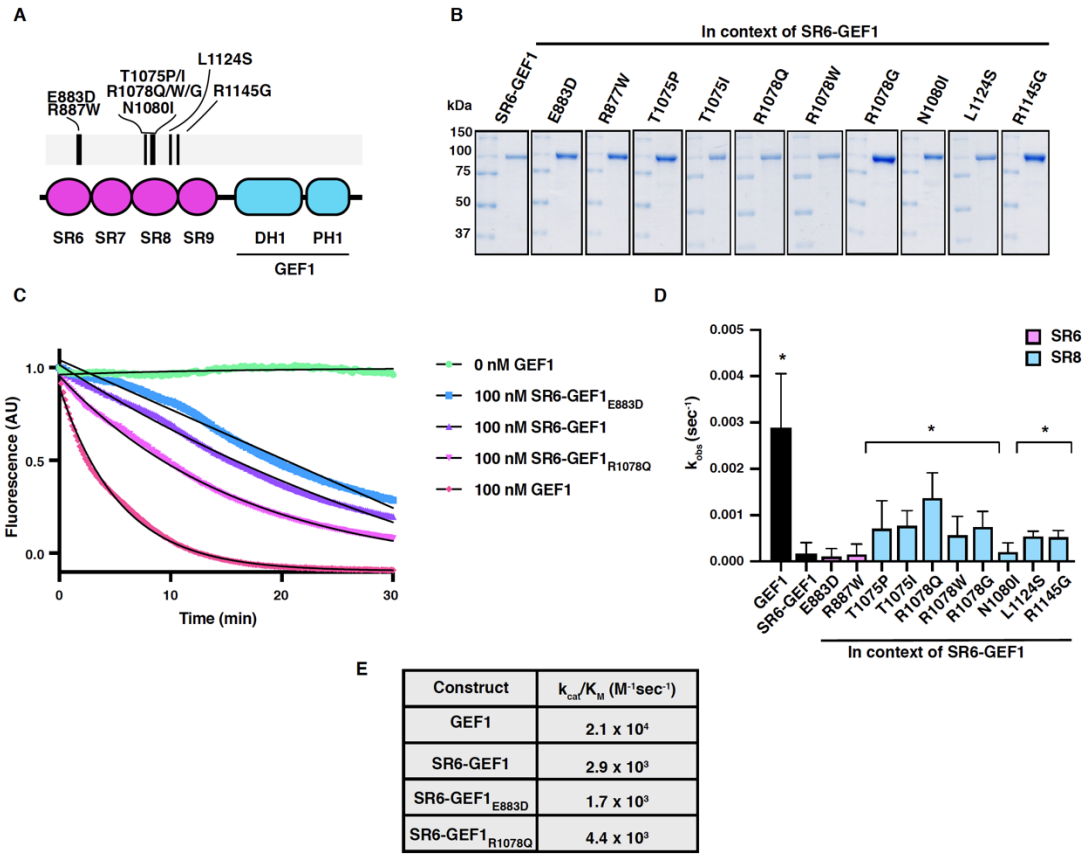

E

Construct	k_{cat}/K_M ($M^{-1}sec^{-1}$)
GEF1	2.1×10^4
SR6-GEF1	2.9×10^3
SR6-GEF1$_{E883D}$	1.7×10^3
SR6-GEF1$_{R1078Q}$	4.4×10^3

Fig. 2.2 Mutations in SR6 and SR8 differentially impact GEF1 activity. *Figure adapted from Bircher, Corcoran et al., 2022*

(A) Schematic of disease associated mutations in the SRs used in this study. (B) Mutants were generated in the context of SR6-GEF1 and purified. (C) Sample GEF assay traces of SR6-GEF1$_{E883D}$ and SR6-GEF1$_{R1078Q}$. Traces in color, exponential fits overlaid in black. (D) SR8 variants in SR6-GEF1 have significantly enhanced catalytic rates, k_{obs}, at equal molar amounts (100 nM) (except N1080I). * = significantly different from SR6-GEF1, $p \leq 0.05$ in an unpaired T-test (n=3) (E) Catalytic efficiency (k_{cat}/K_M) of representative SR6/8 mutants was determined by measuring the k_{obs} values at different (Figure legend continued on next page)

(Figure legend 2.2 continued) concentrations of GEF, as shown in Fig. 1*D*. The catalytic efficiency of SR6-GEF1$_{R1078Q}$ is ~1.5-fold greater than that of SR6-GEF1, while that in SR6-GEF1$_{E883D}$ is ~2-fold slower (n=2). Values for GEF1, SR6-GEF1 from Fig. 1 are shown again for reference, and all are reported as an average of two independent replicates.

catalytic efficiency over WT SR6-GEF1 (Fig. 2.2*E*). Intriguingly, the SR6 variant SR6-GEF1$_{E883D}$ had a *decreased* catalytic efficiency of a k_{cat}/K_M = 1.7 x 10^3 M^{-1} s^{-1}, approximately 50% lower than WT SR6-GEF1 (Fig. 2.2*E*). These findings indicate that NDD-associated variants in SR8 are sufficient to relieve SR autoinhibition.

GEF1 variant D1368V increases GEF activity only in the context of SR6-GEF1.

Hypothesizing that the SRs might contact GEF1 to impact catalytic activity, we searched for GEF1 domain variants that might impact potential autoinhibition of GEF1 activity by SRs. Unlike GEF1 disease variants that lie in the GEF1:Rac1 interface and *decrease* GEF1 activity (101,120,122), D1368V lies in the DH domain but is distal to the GEF1:Rac1 interface, so its impact is less well understood (Fig. 2.3*A*). However, a recent study demonstrated that introduction of the D1368V variant greatly potentiated the ability of the Trio9 splice isoform, which contains all of the SRs, to increase activity of a Rac1 reporter in cells (101). We introduced D1368V into SR6-GEF1, and found that it significantly increased catalytic activity, with a k_{obs} = 1.21 ± 0.3 x 10^{-3} s^{-1} and k_{cat}/K_M = 5.1 x 10^3 M^{-1} s^{-1} (Fig. 2.3, *B-E)*, a 1.75-fold increase over the k_{cat}/K_M for WT SR6-GEF1. In contrast, introducing D1368V into GEF1 alone did not impact its activity compared to GEF1 (Fig. 2.3, *B-E*), indicating that the activating effects of D1368V require SRs 6-9. Together with data reported above, these are consistent with a model in which NDD-associated variants in SR8 and GEF1 relieve inhibition of GEF1 activity by the SRs.

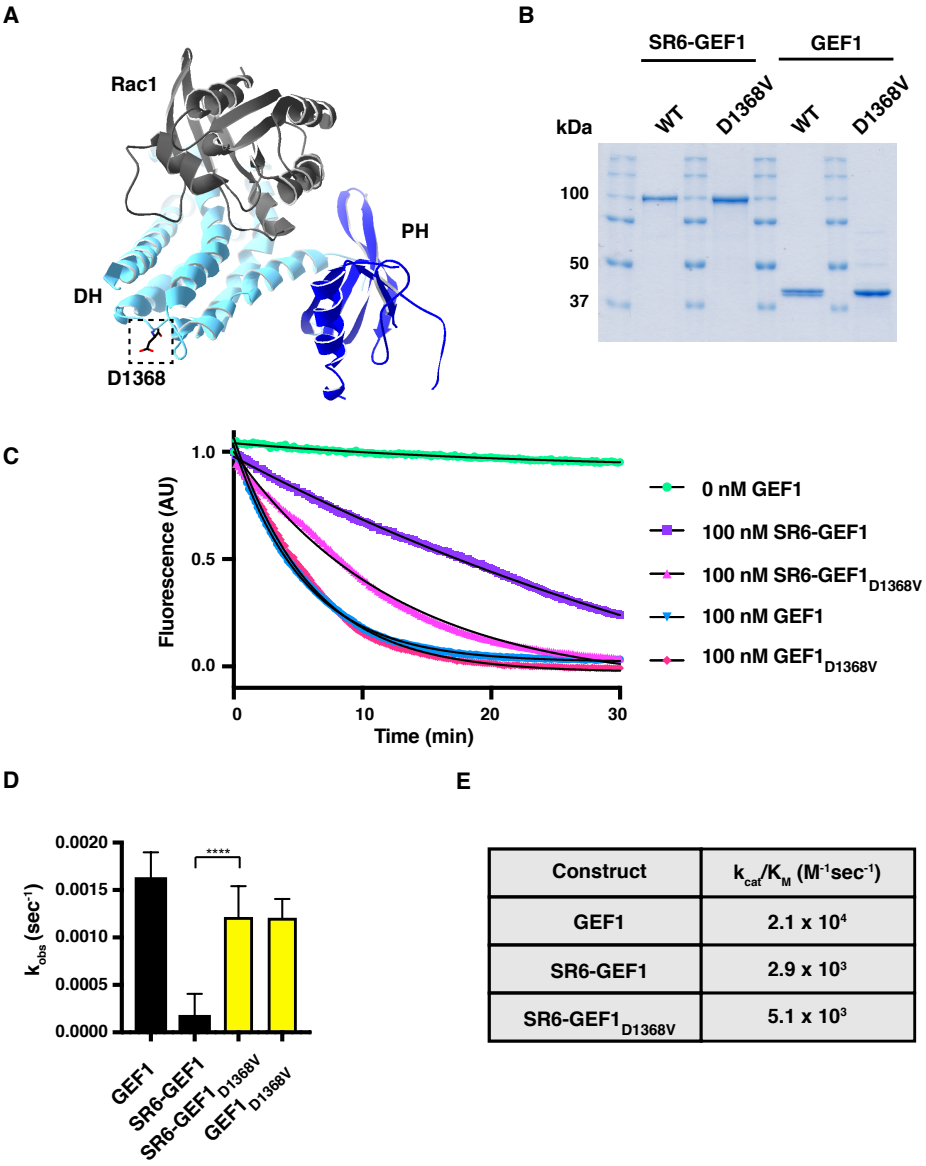

Construct	k_{cat}/K_M ($M^{-1}sec^{-1}$)
GEF1	2.1×10^4
SR6-GEF1	2.9×10^3
SR6-GEF1$_{D1368V}$	5.1×10^3

Fig. 2.3 GEF1 variant D1368V increases GEF1 activity in the context of SR6-GEF1. *Figure adapted from Bircher, Corcoran et al., 2022*

(A) Crystal structure of Trio GEF1 (light and dark blue) and Rac1 (grey), accessed in PDB, ID = 2NZ8 (20). D1368, identified in the box, is distal to the Rac1 binding interface. (B) Samples (approximately 5 µg) of purified components were analyzed by (Figure legend continued on next page)

(Figure legend 2.3 continued) SDS-PAGE and stained with Coomassie Blue R250 to assess purity. Gel bands for WT SR6-GEF1 and WT GEF1 are the same as shown in Fig. 1*B.* (C) Sample GEF assay traces of D1368V in the context of SR6-GEF1 and GEF1. Traces in color, exponential fits overlaid in black. (D) D1368V in SR6-GEF1 increases catalytic rate, k_{obs}, at equal molar amounts of GEF, but has no impact when inserted into GEF1 alone (**** = $p \leq 0.0001$, unpaired T-test for mutant vs WT in respective GEF1 or SR6-GEF1, n=3). (E) Catalytic efficiency (k_{cat}/K_M) of SR6-GEF1$_{D1368V}$ was determined by measuring the k_{obs} values at different concentrations of GEF. Values for GEF1 and SR6-GEF1 shown again for reference. The catalytic efficiency, k_{cat}/K_M, of SR6-GEF1$_{D1368V}$ is ~1.75-fold greater than that of SR6-GEF1 (n=2).

The SRs and GEF1 form distinct stable interacting domains.

We used AlphaFold (126) to model *Drosophila* Trio, which is 48% identical to human Trio from the Sec14-GEF1 domains, and 54% identical to human Trio in SR6-GEF1 (Fig. 2.4*A*). Strikingly, the predicted structure has the SRs curving around the GEF1 domain, with SR8 closely apposed to GEF1 and the NDD-associated mutations concentrated at this SR8:GEF1 interface. This model of SR6-GEF1 and additional analysis using DISOPRED predicted the existence of an unstructured loop between SR9 and GEF1, suggesting this flexible region may be capable of mediating interactions between the SRs and GEF1 (Fig. 2.4*B*) (127). We used limited proteolysis to probe for the presence of a flexible linker between the SR9 and the GEF1 domain that might be susceptible to partial proteolysis. Treatment of SR6-GEF1 at intermediate levels of trypsin yielded two major bands, identified by mass spectrometry as composed of SRs 6-9 and GEF1, respectively. This observation indicates that SRs 6-9 and the GEF1 domain each make up distinct folding units with increased relative resistance to protease (Fig. 2.4*C*). Together, these findings support a model in which the SRs fold over to make contact with GEF1.

To test directly for possible interactions between the SRs and GEF1 domain, we incubated SR6-GEF1 with an 11.4 Å spacer lysine crosslinker, BS3 (bis(sulfosuccinimidyl)suberate), and analyzed crosslinked peptides via mass spectrometry to identify sites in close enough proximity to crosslink. Several long-distance crosslinks were observed between the SRs and the GEF1 domain; specifically, crosslinks between SR8 and the pleckstrin homology (PH) domain

were detected (Fig. 2.4*D*). Additionally, sites of NDD-associated variants in SR8, including amino acids T1075 and L1124, were among peptides crosslinked to GEF1, whereas those in SR6 displayed no crosslinks. Furthermore, Y1532 in the PH domain was contained in a crosslinked peptide to SR8; this residue makes contacts with the substrate Rac1 with the help of H1470 in the DH domain (originally listed as Y1472 and H1410 in the crystal structure (Fig. 2.5*A*) (20)). These results suggest that these residues, which normally make contact with Rac1, are occluded by interactions with the SRs. Overall, these observations are consistent with long-range contact between the SRs and GEF1, and that sites of NDD-associated variants in SR8 may directly contribute to this interaction.

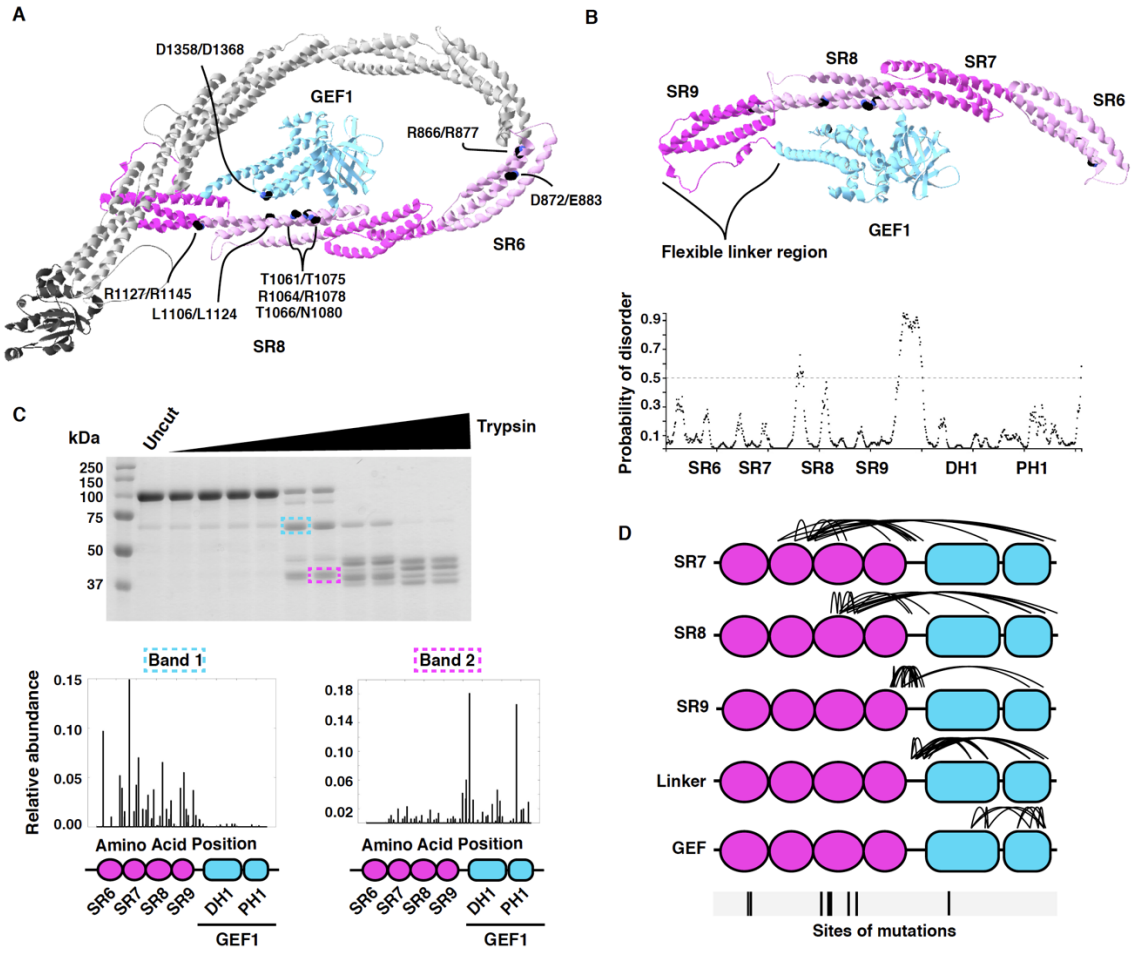

Fig. 2.4 SRs and GEF1 form independent folding units, and SRs interact with GEF1. *Figure adapted from Bircher, Corcoran et al., 2022*

(A) Alphafold model of *Drosophila* Trio, from Sec14-GEF1. Sec14 in dark gray, SR1-5 in light gray, SR6,8 in light pink, SR7,9 in dark pink, GEF1 in blue. Homologous mutations used in this study are modeled as black spheres, with amino acids labeled as *Drosophila*/human. This model predicts an interaction between SR8 and GEF1. (B) SR6-GEF1 only from Alphafold model, rotated to view flexible linker region between GEF1 and SR9. Probability of disorder was predicted using DISOPRED. The region (Figure legend continued on next page)

(Figure legend 2.4 continued) between SR9 and DH1 has high probability of being disordered (cutoff >0.5). (C) Limited proteolysis of SR6-GEF1. His-SR6-GEF1 was incubated with increasing concentrations of trypsin and select bands were identified using mass spectrometry. Relative abundance of identified peptides was plotted to determine composition of each band. SR6-9 and GEF1 form distinct stable domains. (D) SR6-GEF1 was incubated with lysine crosslinker BS3 and crosslinked peptides were identified using mass spectrometry. Each curved line is a uniquely identified peptide. Crosslinks were separated based on their N-terminal crosslink site and categorized based on domain. SR6 is not shown because no crosslinked peptides originating in SR6 were detected. Sites of mutations used in the study shown below for reference. Multiple crosslinks were observed between the SRs and GEF1 domain, indicating that the SRs interact directly with the GEF1 domain.

The SRs reduce GEF1 binding to Rac1.

Dbl family GEF domains all contain a PH domain, which interacts with protein and lipid binding partners to enhance the guanine nucleotide exchange catalytic activity of the DH domain (Fig. 2.5*A*) (20). We hypothesized that an interaction between SRs 6-9 and PH1 may impair the ability of GEF1 to bind Rac1. We used BioLayer Interferometry to measure the association of nucleotide free Rac1 with His-GEF1 or His-SR6-GEF1 immobilized on a Ni-NTA affinity chip. GEF1 bound to Rac1 with a K_d = 151 ± 49 nM in nucleotide-free conditions (Fig. 2.5, *B* and *C*). SR6-GEF1 had a reduced affinity for Rac1, with a K_d = 316 ± 87 nM (Fig. 2.5, *B* and *C*). Taken together with the crosslinking data, this supports a model where the SRs contact the PH domain to impair GEF1 binding to Rac1, which likely contributes to the reduction in observed GEF1 activity.

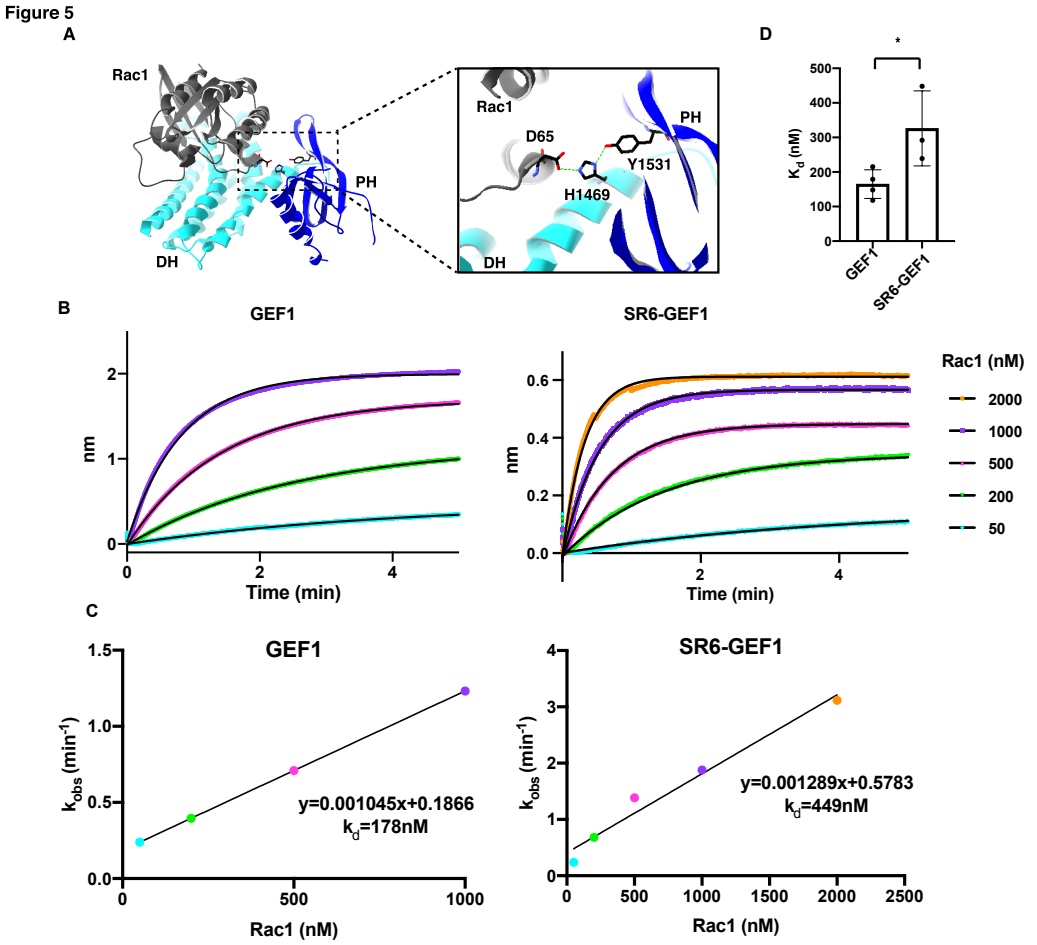

Fig. 2.5 Inclusion of SRs 6-9 reduce binding to Rac1. *Figure adapted from Bircher, Corcoran et al., 2022*

(A) Crystal structure of GEF1 (light and dark blue) and Rac1 (dark grey)(from PDB, ID = 2NZ8 (20). The Trio PH domain Y1535 hydrogen bonds with Trio DH domain H1470 to stabilize an interaction with D65 in Rac1 (expanded box). (B) His-GEF1 or His-SR6-GEF1 were immobilized on an Ni-NTA biosensor and the association of different concentrations of Rac1 was measured. Representative traces shown, with data in color and one phase exponential fits in black. (Figure legend continued on next page)

Full concentration gradients (4-5 Rac1 concentrations) were performed at least three independent times and used to calculate a K_d. (C) Each association curve was fit to a one-phase exponential curve to get a k_{obs} value. Each k_{obs} value was plotted against Rac1 concentration and a linear fit was used to obtain k_{on} and k_{off} values, used to compute a k_d. Representative values from the association curves in (C) shown. (D) The k_d of GEF1 or SR6-GEF1 binding to Rac1 values obtained from linear fits in (C). SR6-GEF1 has a 2-fold weaker affinity for Rac1 than GEF1 (* = $p \leq 0.05$, unpaired t-test).

SRs 6-9 inhibit GEF1-induced cell spreading.

Trio GEF1 activates Rac1 to coordinate downstream cytoskeletal changes and mediate changes in cell morphology (3,5,21,128). We first expressed Trio GEF1-GFP in HEK293 cells and quantified its impact on cell morphology (Fig. 2.6, *A*-*C*). When matched for GFP expression levels, GEF1 expressing cells had significantly increased cell area compared to GFP controls (Fig. 2.6, *A*-*C)*. Cells expressing GEF1 appeared to be more spread, with round lamellipodia encompassing the cell edge, a common result of Rac1 activation (Fig. 2.6*B*). Cells that expressed a catalytic-dead mutant of GEF1, GEF1 ND/AA (N1465A/D1466A), had indistinguishable area compared to the GFP controls, indicating a key role for GEF1 catalytic activity in this morphological change (129). In contrast to GEF1, SR6-GEF1 expressing cells had no measurable effect on cell area, but the SR8 mutant SR6-GEF1$_{R1078Q}$ increased cell area over that of GFP and SR6-GEF1 WT (Fig. 2.6, *B* and *C*). Cells expressing SR6-GEF1$_{R1078Q}$ also appeared similar in morphology to those cells expressing GEF1 alone, with more full, rounded edges (Fig. 2.6*B*). In sum, inclusion of SRs 6-9 inhibits GEF1 activity in cells, impacting downstream Rac1-dependent characteristics like cell morphology, and disease-associated variants can disrupt this inhibitory regulation.

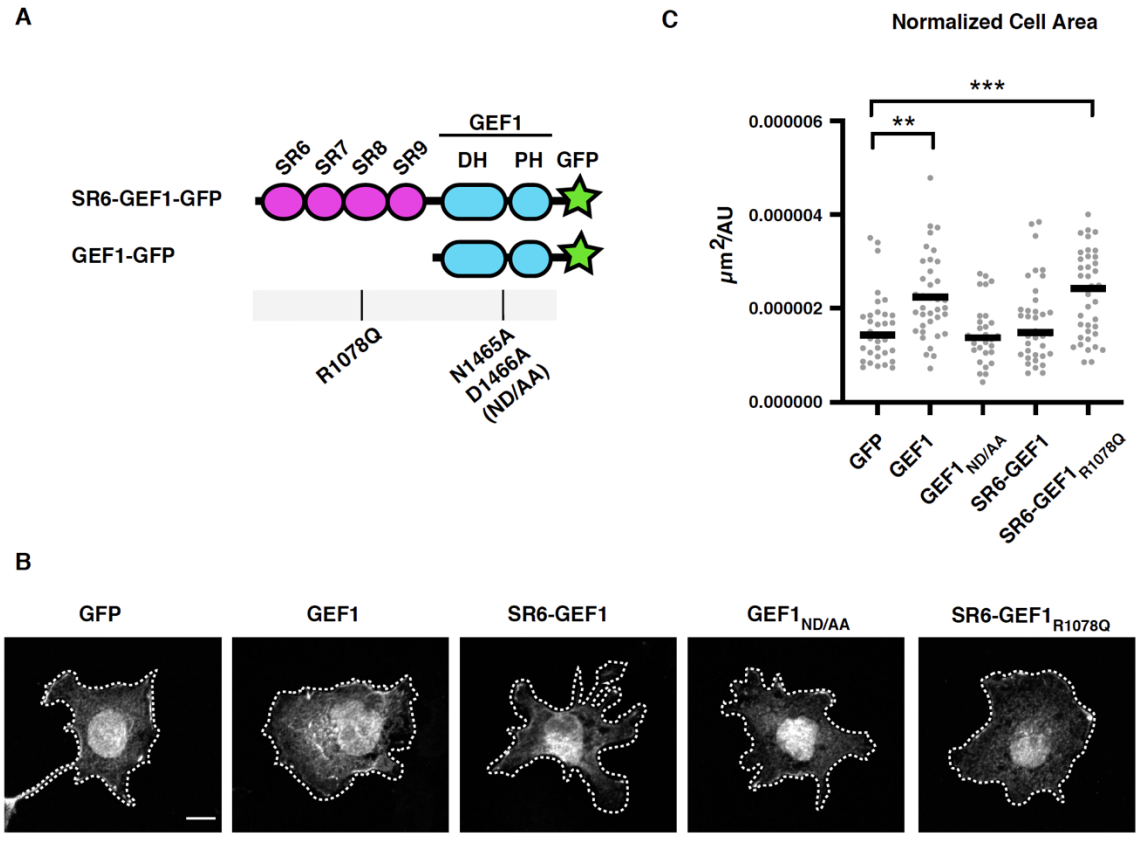

Fig. 2.6 SRs 6-9 reduce the impact of GEF1 on cell spreading. *Figure adapted from Bircher, Corcoran et al., 2022*

(A) Schematic of constructs used, with mutants shown below. (B) Constructs in A were transfected into HEK293 cells and plated on fibronectin. Cells were fixed and stained using anti-GFP to visualize GFP expression and cell morphology. Cells expressing GEF1 and SR6-GEF1 R1078Q appeared to have more rounded edges and circular shapes. Scale bar = 10 μm. (C) Cell area, normalized to protein expression on a cell-by-cell basis, was quantified. Cell area increased upon expression of GEF1 and SR6-GEF1$_{R1078Q}$, while expression of a catalytic-dead GEF1 mutant (ND/AA) or (Figure legend continued on next page)

(Figure legend 2.6 continued) SR6-GEF1 had no effect compared to GFP alone. Contrast adjusted between images shown to best visualize cell edge; cell edge outlined with white dashed line. One biological replicate was performed, 30-40 cells were analyzed per group (** = $p \leq 0.01$, *** = $p \leq 0.001$, unpaired t-test between GFP control and each group).

2.3 Discussion

We provide evidence here that the Trio SRs 6-9 directly inhibit GEF1 activity via intramolecular interactions in vitro and in cells. We demonstrate that NDD-associated variants in the SR8 domain and GEF1 release this autoinhibitory constraint, strongly suggesting that disruption of this GEF1 regulatory mechanism contributes to the pathophysiology of these disorders. Using chemical cross-linking and BioLayer Interferometry, we show that the SRs primarily contact the PH1 region of GEF1, and that contact is associated with reduced binding affinity of Rac1 in vitro. Our results provide a novel mechanism by which the Trio SRs autoinhibit the RhoGEF Trio in vitro and in cells. This discovery offers insight into how a key Trio function is regulated, making it a potential target for therapeutic intervention.

Inclusion of Trio SRs autoinhibit GEF1 activity in vitro and in cells.

Previous cell-based studies have shown that removing the SRs is associated with increased downstream Rac1 activity and Trio gain-of-function phenotypes in vivo, suggesting that the Trio SRs function to inhibit GEF1 activity (36,77,124). This hypothesis is supported by evidence that other RhoGEFs, like Tiam1, contain autoinhibitory N-terminally adjacent accessory domains (37,124,130). In most cases, how autoinhibition occurs and how it is released to activate GEF activity is unknown. Our results show that inclusion of SRs significantly decreases GEF1 catalytic activity in vitro and inhibits GEF1-dependent processes in cells,

suggesting that the SRs are sufficient to inhibit GEF1 activity via intramolecular interactions.

SRs make direct contact with PH region of GEF1 and impair interactions with Rac1.

Within GEF1, the DH1 domain contains the interface that promotes GTP exchange onto Rac1 and this is enhanced by the presence of the PH1 domain (17,22). Indeed, crystal structures of the Trio GEF1 domain (20) show that Y1532 in the PH domain complexes with H1470 in the DH domain to interact with Rac1. Using chemical crosslinking, we demonstrate that SRs 7-9 contact the GEF1 PH domain. Mapping these crosslinked sites onto the GEF1 crystal structure strongly suggest that the SRs contact a peptide in the PH domain that contains Y1532 (20). However, chemical crosslinking lacks the resolution to determine whether the SR:PH interaction *sterically* blocks contact with Rac1 or works via an *allosteric* mechanism, preventing the PH domain from engaging Rac1. In addition, whereas our catalytic rate measurements suggest a 90% decrease in activity, we observed only a 50% decrease in SR6-GEF1 binding affinity for Rac1 in a nucleotide free state, compared to GEF1 alone. We propose that this is because engagement of the SRs with GEF1 impairs other steps in the catalytic cycle, as demonstrated by our catalytic efficiency data, rather than solely impacting binding affinity for Rac1. Future studies will elucidate whether other components of the nucleotide exchange process are impacted by the SRs.

NDD associated mutations in SR8 and GEF1 disrupt SR-mediated GEF1 inhibition.

Two rare variant clusters in *TRIO*, one in SR8 (Fig. 2*A*) and one in GEF1, have been linked to distinct endophenotypes in individuals with NDDs (121). For example, *TRIO* SR8 variants are linked to developmental delay and macrocephaly in humans and cause increased Rac1 (GEF1) activity in cells, whereas most mutations in the GEF1 domain are linked to mild intellectual disability, microcephaly, and reduced Rac1 activity in cells. However, how SR8 variants increased Rac1 activity was completely unknown. We hypothesized that the increased Rac1 activity associated with SR8 domain variants resulted from disruption of SR-mediated GEF1 inhibition. We generated mutant SR6-GEF1 constructs harboring distinct disorder-associated variants and found that nearly all SR8 mutants increased SR6-GEF1 catalytic activity 3-7 fold. Interestingly, the one exception, N1080I, disrupts binding to neuroligin-1 and blocks neuroligin-1 mediated synaptogenesis (131), suggesting that this mutation involves the disruption of an entirely different regulatory mechanism. Interestingly, N1080I is not reported to have less severe or distinct phenotypes compared to the bulk of the other SR8 mutations (121). We hypothesize that other sites, including N1080I, in the SRs serve as convergence points for upstream activators to regulate GEF1 activity, and discuss this idea in Chapter 3. Together, these data demonstrate that many NDD variants in SR8 are sufficient to relieve SR-mediated GEF1 inhibition.

We also found that a GEF1 domain variant associated with Rac1 activation in cells likely impacts SR-mediated GEF1 inhibition. Unlike GEF1 disease variants that sit

in the Rac1 interface and *decrease* GEF1 activity, this variant, D1368V, is distal to the Rac1 interface and *hyperactivates* Rac1 activity in cells when introduced in the Trio9S isoform (131) (101,120,122). Our results indicate that D1368V significantly increases GEF1 activity in the context of SR6-GEF1 but has no effect on GEF1 alone. We propose that D1368V enhances SR6-GEF1 activity by disrupting SR autoinhibition. Indeed, modeling (Fig. 2.4*A*) predicts that the SR8 domain interacts with GEF1, and the activating SR8 and GEF1 variants lie at the interface of these two domains.

NDD-associated variants in SR6 may reinforce SR-mediated GEF1 inhibition.

We also generated two SR6-GEF1 constructs harboring individual disease variants in the SR6 domain, whose impact on Trio function remains completely unknown. While the rate constant (k_{obs}) values obtained for each construct did not significantly decrease compared to WT SR6-GEF1, trends in the nucleotide exchange assays suggested exchange may be slower. We hypothesized that using a one-phase exponential decay fit to obtain the rate constant of each GEF construct at a single concentration (100 nM) was not precise enough to detect a significant measurement. Therefore, we measured the k_{obs} over a span of GEF concentrations and obtained the catalytic efficiency from a linear fit (Fig. 2.1*D*). Measurement of catalytic efficiency, k_{cat}/K_M, of both wild-type SR6-GEF1 and SR6-GEF1$_{E883D}$ revealed that SR6-GEF1$_{E883D}$ is decreased 2-fold compared to wild-type SR6-GEF1. This suggests that NDD-associated variants in SR6 *decrease* GEF1 activity. While the explanation for this result is unclear, one possibility is that SR6 acts as a hinge region allosterically governing the flexibility of the helices

surrounding SR8, and that SR6 variants may decrease the ability for the SRs to release their inhibitory lock on the GEF1 domain. In addition, it is unknown how the severity of phenotypes associated with the SR6 mutations compare to those of the SR8 mutations. These observations highlight the importance of understanding how complex upregulation and downregulation of Trio GEF1 activity contributes to NDDs.

The SRs may serve as a target for activators of Trio GEF1 activity.

We demonstrated that the SRs inhibit Trio GEF1 activity, but it is unclear how inhibition may be released in a cellular context. SR domains are widely accepted as scaffolding proteins that coordinate cytoskeletal interactions with high spatial precision. Considering that Trio is known to act downstream of cell surface receptors to coordinate cytoskeletal rearrangements, we anticipate that the Trio SRs serve as a target of interaction partners to engage and activate Trio GEF1 activity in cells. Trio SRs interact with diverse cellular partners, including synaptic scaffolding proteins (Piccolo and Bassoon) (132), cell-adhesion molecules (VE-cadherin and Intercellular Adhesion Molecule 1 (ICAM1)) (88,93), and membrane trafficking proteins (RABIN8) (52). These SR binding partners may engage Trio to coordinate GEF1 activation and/or deactivation in a spatiotemporal manner. Indeed, several studies have shown that Trio interactions with binding partners impacts Rac1 activity in cells (88,93,131,133) (65). For example, VE-cadherin, directly binds Trio SR5 and SR6, and this interaction locally increases Rac1 activity in cells (88). Similarly, the ICAM1 intracellular tail directly binds Trio GEF1, and the Trio/ICAM1 interaction potentiates ICAM1 clustering at adhesion sites,

promoting Rac1 activation in cells (93). Finally, the integral membrane protein Kidins220 regulates Rac1-dependent neurite outgrowth via interactions with the Trio SRs (133). While these studies suggest that the Trio signaling partners may engage and activate Trio GEF1 activity, the specific interaction interfaces and binding stoichiometry that mediates GEF1 activation and how they are impacted by disorder-associated variants is presently unknown. Based on our evidence that SR8 variants relieve an autoinhibitory constraint, we anticipate that SR8 may be a convergence point for upstream activators and coordinated regulation of GEF1 activity.

Conclusions

TRIO has emerged as a significant risk gene for NDDs. Using biochemical and genetic tools, we identified a novel regulatory mechanism by which Trio SRs inhibit GEF1 activity and showed that disorder-associated variants are sufficient to relieve this autoinhibitory constraint. This discovery will serve as a model to understand how Trio GEF1 is regulated by physiological signals and how its disruption leads to NDDs. This mechanism may also offer a new target for therapeutic interventions for *TRIO*-associated NDDs.

2.4 Methods

Expression construct cloning and protein purification

Human Trio SR6-GEF1 was PCR amplified and inserted into the pFastBac1 HTa vector (Invitrogen). Site directed mutagenesis was used to insert point mutations

into pFastBac1-Hta-SR6-GEF1 construct and confirmed by DNA sequencing. Primers used for cloning are included in Table 2.1.

Recombinant baculoviruses were generated using Sf9 cells in the Bac-to-Bac expression system (Thermo Fisher Scientific). Baculoviruses were used to infect Hi5 cells at an estimated multiplicity of infection = 1 for 48 hours before lysis in lysis buffer (20 mM HEPES pH 7.25, 500 mM KCl, 5 mM β-mercaptoethanol (BME), 5% glycerol, 1% Triton X-100, 20 mM imidazole, 1 mM DTT, 1 mM phenylmethylsulfonyl fluoride (PMSF), 1x Roche cOmplete protease inhibitors EDTA free) for 20 min at 4°C. Lysates were affinity purified using nitrilotriacetic acid (Ni-NTA) resin (Qiagen) and eluted with 250 mM imidazole. Elution fractions were further purified over a Sephadex 200 (S200) Increase 10/300 GL column into assay buffer (20 mM HEPES pH 7.25, 150 mM KCl, 5% glycerol, 0.01% Triton X-100, 1 mM DTT), aliquoted, and flash frozen in liquid Nitrogen for long-term storage at -80°C.

Human Trio GEF1 and Rac1 were generated and affinity purified from bacterial cells as described in Blaise et al. (125). Point mutants were generated using site-directed mutagenesis. Following affinity purification, eluted protein was further purified over an S200 increase column into assay buffer, aliquoted and flash frozen for long-term storage. Stokes radii of proteins were estimated based on the elution volume from the S200 increase column, calculated based on a standard curve generated by running protein standards (Protein Standard Mix 15-600kDa, Supelco).

TABLE 2.1 PRIMER SEQUENCES AND VECTORS USED FOR GENERATING GEF1 AND SR6-GEF1 CONSTRUCTS. *TABLE ADAPTED FROM BIRCHER, CORCORAN ET AL., 2022*

construct	nt change	primer seq fwd (5'-3')	primer seq rev (5'-3')	vector
R877W	c2629t	AGAGATGTAGACATGGCAACTTGGGTCCAGGAC	GTCCTGGACCCAAGTTGCCATGTCTACATCTCT	pFb-HTA
T1075I	c3224t	TTCCTGAAGGCTTGCATCCTTGCTCGGAGG	CCTCCGAGCAAGGATGCAAGCCTTCAGGAA	pFb-HTA
T1075P	a3223c	CCTGAAGGCTTGCCCCCTTGCTCGGAG	CTCCGAGCAAGGGGGCAAGCCTTCAGG	pFb-HTA
R1078W	c3232t	GGCTTGCACCCTTGCTTGGAGGAATGCAG	CTGCATTCCTCCAAGCAAGGGTGCAAGCC	pFb-HTA
R1078G	c3232g	GGCTTGCACCCTTGCTGGGAGGAATGCAG	CTGCATTCCTCCCAGCAAGGGTGCAAGCC	pFb-HTA
R1078Q	g3233a	CTTGCACCCTTGCTCAGAGGAATGCAGACGT	ACGTCTGCATTCCTCTGAGCAAGGGTGCAAG	pFb-HTA
R1145G	a3433g	TACGTGGTCTTTGAGGGGAGTGCCAAGCAGG	CCTGCTTGGCACTCCCCTCAAAGACCACGTA	pFb-HTA
E883D	g2649t	GTCCAGGACCTGCTGGATTTTCTTCATGAAAAACAG	CTGTTTTTCATGAAGAAAATCCAGCAGGTCCTGGAC	pFb-HTA
D1368V	a4103t	gtaacaaaacaatgtccaacaacctctggcaactgttcatatt	aatatgaacagttgccagaggttgttggacattgttttgttac	pFb-HTA
SR6-GEF1	WT	GATCGAATTCCTGCGCATCTTCGAGAGGGAC	GATCCTCTAGActaTTTCCCTTCAGGTGGATCGT	pFb-HTA
N1080I	a3239t	gaagacgtctgcaatcctccgagcaagggt	accctgctcggaggattgcagacgtcttc	pFb-HTA
L1124S	t3371c	tggtccagtaatgcgataccctgttctcccgttg	caacgggagaacagggtatcgcattactggacca	pFb-HTA
GEF1	see Blaise et al, 2021			pET-His-TT
Rac1	see Blaise et al, 2021			pGEX-6P1
px1-GEF1-GFP	WT	GATCGTTAACGGCTCAGAGGTGAAACTTCGAGATGCTGCTCATG	GATCGCGGCCGCTCCCTTCAGGTGGATCGTCCGCTCCTGGATGA	px1-HA-GFP
px1-SR6-GEF1-GFP	WT	GATCGTTAACCTGCGCATCTTCGAGAGGGACGCCATCGACAT	GATCGCGGCCGCTCCCTTCAGGTGGATCGTCCGCTCCTGGATGA	px1-HA-GFP
px1-GEF1-GFP ND/AA	/a4397c/t4398c	GTG CCG AAG CGA GCC GCT GCC GCC ATG CAC CTC AG	CTG AGG TGC ATG GCG GCA GCG GCT CGC TTC GGC AC	px1-HA-GFP

BODIPY-FL-GDP nucleotide exchange assays

12.8 μM Rac1 was loaded with 3.2 μM BODIPY-fluorescein (FL)-GDP (Invitrogen) in 1X assay buffer (20 mM HEPES pH 7.25, 150 mM KCl, 5% glycerol, 1 mM DTT, 0.01% Triton X-100) plus 2 mM EDTA to a total volume of 25 μL per reaction, then incubated for 1 hour at room temperature. BODIPY-FL-GDP loading onto Rac1 was halted by the addition of 5 μL 30 mM $MgCl_2$ per reaction for a total reaction volume of 30 μL and final $MgCl_2$ concentration of 5 mM. Prior to initiating the reaction with 100 nM Trio GEF, 30 μL of GTPase (12.8 μM) plus $MgCl_2$ (5 mM) mix or blank (3.2 μM BODIPY-FL-GDP, 2 mM EDTA, and 1X assay buffer) was added to appropriate wells. During this incubation period, GEF1-containing proteins were prepared in 1X assay buffer, 4 mM GTP, and 2 mM $MgCl_2$. Exchange reactions were initiated by adding 10 μL of 100 nM Trio GEF mixture (as stated above) to each well, for a total reaction volume of 40 μL. Real-time fluorescence data was measured every 10 seconds for 30 min monitoring BODIPY-FL fluorescence by excitation at 488 nm and emission at 535 nm, as per Blaise et al. (125).

All catalytic exchange data are representative of at least three independent replicates. Results are shown as the mean ± standard deviation (SD) from multiple experiments. Unpaired t-tests were used to determine statistical significance (two-tail p-value <0.05). Catalytic efficiencies (k_{cat}/K_M) of select GEF constructs were extracted from a linear fit of catalytic rate (k_{obs}, sec^{-1}) vs. GEF1 concentration (nM).

Two technical replicates were performed for each GEF construct, and the catalytic efficiency values were averaged.

Protein structure predictions

AlphaFold was used to access the predicted structure of *Drosophila* Trio, entry number AF-Q7KVD1-F1 (126). Mutations in human Trio were mapped onto the AlphaFold structure using a protein-protein alignment of full-length *Drosophila* and human Trio. DISOPRED was used to predict the probability of disorder of Trio SR6-GEF1, amino acids 788-1599 (127).

Limited proteolysis

SR6-GEF1 in 1X assay buffer plus 10 mM $CaCl_2$ was diluted to 0.4 mg/mL and incubated with increasing concentrations of trypsin (0.001 mg/mL to 0.11 mg/mL) for 1 hour at room temperature in a 25 µL total reaction volume. Reactions were quenched with 8 µL quench buffer (50 mM Tris-HCl pH 6.8, 4% SDS, 10% glycerol, 0.1% bromophenol blue, 5% BME, 1 mM PMSF, 4 mM EGTA, 4 mM EDTA) and immediately boiled for 10 minutes. Samples were immediately run on a 12% SDS-PAGE gel, and proteins were visualized by Coomassie R250 staining.

Major gel bands were excised and washed with 50:50 acetonitrile:water buffer containing 100 mM ammonium bicarbonate. Proteins in the gel were reduced with 4.5 mM DTT at 37°C for 20 min and alkylated with 10 mM iodoacetamide at room temperature for 20 minutes in the dark. Gel bands were washed twice with 50:50 acetonitrile:water containing 100 mM bicarbonate and dried for 10 min in a

SpeedVac. Trypsin digestion was carried out (1:100 molar ratio of trypsin to protein) by incubation with the gel piece at 37°C overnight. The digest samples were analyzed by LC–MS/MS using a Q-Exactive Plus mass spectrometer (ThermoFisher) equipped with a Waters nanoACQUITY ultra-performance liquid chromatography (UPLC) system using a Waters Symmetry C18 180 µm by 20 mm trap column and a 1.7 µm (75 µm inner diameter by 250 mm) nanoACQUITY UPLC column (35°C) for peptide separation (Waters). Trapping was done at 15 µL/min with 99% buffer A (100% water, 0.1% formic acid) for 1 min. Peptide separation was performed at 300 nL/min with buffer A and buffer B (100% acetonitrile, 0.1% formic acid) over a linear gradient. High-Energy collisional dissociation was utilized to fragment peptide ions via data-dependent acquisition. Mass spectral data were processed with Proteome Discoverer (v. 2.3) and protein database search was carried out in the Mascot search engine (Matrix Science, LLC, Boston, MA; v. 2.6.0). Protein searches were conducted against the *Trichoplusia ni* protein database and the human Trio SR6-GEF1 sequence. Mascot search parameters included: parent peptide ion tolerance of 10.0 ppm; peptide fragment ion mass tolerance of 0.020 Da; strict trypsin fragments (enzyme cleavage after the C terminus of K or R, but not if it is followed by P); fixed modification of carbamidomethyl (C); and variable modification of phospho (S, T, Y), oxidation (M), and Propioamidation (C), and Deamidation (NQ). Peptide identification confidence was set at 95% confidence probability based on Mascot MOWSE score. Results were transferred to Scaffold software (Proteome Software, Portland, OR; v. 4) for further data analysis to look at peptide abundances in

reference to their start position. These were utilized to plot in a frequency distribution to determine band identity.

Crosslinking mass spectrometry

Crosslinking experiments were performed as in Sanchez et al. (134) with deviations noted below. 25 µg of protein was incubated in assay buffer with 100 µM BS3 (bis(sulfosuccinimidyl)suberate) (Thermo Fisher) for 30 min on ice. The reaction was quenched by adding Tris pH 7.25 to 10 mM final concentration. Protein was then acetone precipitated and the pellet was alkylated with iodoacetamide and digested with trypsin. Peptides were desalted on a 100 µL Omix C_{18} tip (Agilent), dried, and reconstituted in 100 µL of 0.1% formic acid. Mass spectrometry was performed on an Orbitrap Exploris 480 equipped with an EasySpray nanoESI source, an EasySpray 75 µm x 15 cm C_{18} column, and a FAIMS Pro ion mobility interface coupled with an UltiMate 3000 RSLCnano system (Thermo Scientific). Each sample was analyzed at four different FAIMS compensation voltages (CV= -40V, -50V, -60V, -70V) to provide gas-phase enrichment/fractionation of crosslinked peptide ions (135). Each analysis was a separate injection (2.5 µL sample). The sample was loaded at 2% B at 600 nL/min for 35 min followed by a multi-segment elution gradient to 35% B at 200 nL/min over 70 min with the remaining time used for column washing and re-equilibration (buffer A: 0.1% formic acid (aq); buffer B: 0.1% formic acid in acetonitrile). Precursor ions were acquired at 120,000 resolving power and ions with charges 3-8+ were isolated in the quadrupole using a 1.6 m/z unit window and dissociated by

HCD at 30% NCE. Product ions were measured at 30,000 resolving power. Peak lists were generated using PAVA (in house Python app), searched with Protein Prospector v6.3.23 (136), and classified as unique residue pairs using Touchstone (an in-house R library) at SVM.score ≥1.5 corresponding to a residue pair level FDR < 0.1% and then further summarized and presented as domain-domain pairs using Touchstone. The search database consisted of the human *TRIO* sequence (O75962) and a 10x longer decoy database. Tryptic specificity with 2-missed cleavages and tolerance of 10/25 ppm (precursor/product) were specified along with DSS/BS3 crosslinking for the Prospector search.

BioLayer Interferometry

Kinetic binding assays were performed using a ForteBio BLItz instrument (ForteBio, Sartorius). Ni-NTA biosensors were pre-hydrated in assay buffer for 10 min prior to the experiment. Biosensors were first measured for a baseline signal for 30 seconds before loading His-GEF1 (0.5 μM) or SR6-GEF1 (2 μM) in assay buffer for 5 min (concentrations were optimized for reproducible loading and signal change). Biosensors were then re-equilibrated in assay buffer for 30 seconds before introducing varying concentrations of Rac1 (at least 4 concentrations per experiment) in assay buffer for 5 min to measure association. Association curves were fit to a one phase exponential curve, and rate constants were plotted against Rac1 concentration, and the linear fit of this data was used to calculate a K_d (k_{off} = x-intercept, k_{on} = slope; $k_d = k_{off}/k_{on}$). Concentration gradients were replicated at least three times independently, and the K_d measurements of each interaction

were then compared using an unpaired t-test. Reported values are mean ± standard deviation.

Measurement of GEF and SR6-GEF1 impact on cell morphology

Polyethylenimine was used to transfect HEK293 cells with 0.5-4 µg of DNA in 6-well dishes at a density of $3x10^5$ cells per well. 24 hours after transfection, cells were trypsinized and replated at a density of $2.5x10^4$ cells per coverslip on fibronectin-coated coverslips (10 µg/mL fibronectin). 24 hours post plating, cells were fixed and stained as in Lim et al. (137). Cells were fixed for 5 minutes in 2% paraformaldehyde in cytoskeleton buffer (10 mM MES pH 6.8, 138 mM KCl, 3 mM $MgCl_2$, 2 mM EGTA, 320 mM sucrose). Cells were rinsed 3 times in Tris Buffered Saline (TBS) (150 mM NaCl, 20 mM Tris pH 7.4) and incubated with 5 µg/mL Alexa Fluor Wheat Germ Agglutinin 555 in TBS (Thermo Fisher) for 10 minutes to visualize the cell membrane when imaging. Cells were washed another three times in TBS, then permeabilized for 10 minutes in 0.3% TritonX-100/TBS and washed another 3 times in 0.1% TritonX-100/TBS. Cells were blocked for 30 minutes in antibody dilution buffer (ADB) (0.1% TritonX-100, 2% BSA, 0.1% NaN_3, 10% FBS, TBS) and incubated with primary antibody (ADB containing a 1:2000 dilution of Goat Anti-GFP, Rockland) at 4°C overnight. The next morning, cells were washed in 0.1% TritonX-100/TBS 3 times and incubated in secondary antibody for 1 hour at room temperature (in ADB, 1:2000 Alexa Fluor 488 Donkey Anti-Goat, Abcam). Cells were washed once in 0.1% TritonX-100/TBS, once in TBS, and then mounted onto glass slides using AquaMount (Lerner Laboratories). After drying, coverslips

were sealed using clear nail polish and imaged using a 40x objective on a spinning disk confocal microscope (UltraVIEW VoX spinning disk confocal (Perkin Elmer) Nikon Ti-E-Eclipse), collecting a full z-stack of images for each cell. Identical microscope settings were used between imaging samples.

After imaging cells, images were processed using ImageJ to generate a sum projection of the GFP channel for quantifying fluorescence. Images were then analyzed using CellProfiler to semi-automatically detect cell edges and compute cell area (138). Cell area was normalized for protein expression on a single cell basis by dividing the total area of the cell by the total GFP fluorescence of the cell. Normalized cell area was compared using an unpaired t-test to compare between GFP control and all other groups. One biological replicate was performed and 30-40 cells were quantified per group. Statistical significance was determined using an unpaired t-test between the GFP control and all other groups, with a p-value cutoff <0.05.

Chapter 3

Trio and its interactors in a cellular context

3.1 Overview

This work is currently unfinished and is provided here as a starting point for future studies. The main objective of my work was to open potential avenues to answer fundamental, yet unresolved questions about Trio function in the larger context of the cell. Specifically, it is unclear how the Trio GEF functions are regulated within the cell and how specific intramolecular regulation or interactions with other proteins might affect GEF activity. This cellular perspective on Trio function serves as a nice complement to the predominantly biochemical work I completed in Chapter 2. I took two approaches to answer these questions: (1) generating a *TRIO* KO cell line and (2) identifying potential protein interactors that may impact Trio catalytic activity. Tony Koleske immortalized the *TRIO*$^{fl/fl}$ cell line and Juliana Shaw did work to validate this, originally published in Katrancha et al., 2019. Ellen Corcoran helped design cloning for protein activators. Amanda Jeng designed protein constructs for ADAM23 and L1CAM, and Amanda and Tony purified these proteins.

3.2 Candidate interactors and specific cell signaling pathways

The fundamental question I sought to answer for this part of my thesis was how interactions with candidate proteins might activate Trio GEF function via release of autoinhibitory mechanisms in a spatiotemporal manner. I am particularly interested in release of autoinhibition of GEF1 by the spectrin repeats (follow-up to Chapter 2).

A major class of candidate interactors are proteins whose expression levels change upon loss of Trio, suggesting they may function in the same biochemical pathway. Mass spectrometry was used to analyze proteins whose levels change upon loss of Trio in the mouse motor cortex, and Amanda Jeng later identified ADAM23 and L1CAM as intriguing hits (82). ADAM23 and L1CAM are both synaptic adhesion proteins that are involved in synaptic transmission and neurite outgrowth, respectively (139,140) (Table 3.1).

Another class of candidate activating proteins are those that have been shown to function upstream of Trio and have downstream effects on RhoA or Rac1 activity. The best candidates are proteins that have been shown to interact with Trio in a cellular context or in vitro. Based on these criteria, we were interested in an initial set of proteins: ICAM1, VE-cadherin, Kidins220, and Neuroligin. Interactions involving ICAM1, VE-cadherin, and kidins220 are described in the introduction or cited works (ICAM1 and Kidins220 (93) (133); VE-cadherin and NLGN (Sections 1.4-1.5) (Table 3.1). Significant recent work has further implicated Neuroligin as a strong candidate interactor, summarized below (131) .

The neuroligin family of proteins are synaptic cell adhesion molecules that interact with neurexins to promote the formation of synapses (131). Neuroligin1 co-immunoprecipitates with Trio9 in rat brain homogenate and HEK293 lysate. Trio9 N1080I in HEK cells reduces amount of Neuroligin immunoprecipitated by ~50%. Replacing Trio and Kalirin with Trio9 N1080I in CA1 pyramidal neurons (rat) prevents Neuroligin-induced increases in dendritic spine number and other

downstream effects on glutamatergic synapses (131). Therefore, Neuroligin likely interacts with Trio, and disruption of this interaction reduces the effects of Neuroligin on downstream synaptogenesis. However, it is unknown if Trio interacts directly with Neuroligin, and if Neuroligin signals through Trio to directly promote GEF1 activity (Table 3.1). It is interesting to note that N1080I was the single SR8 variant that had no effect on SR6-GEF1 activity in our Chapter 2 studies. How this variant impacts a direct biochemical interaction will be a very important question to answer.

3.3 *TRIO*$^{fl/fl}$ fibroblast cell line as a model

This preliminary work was performed by Anthony Koleske and Juliana Shaw, and published in Katrancha et al. 2019 (82). I summarize their work here as background.

Several nonsense mutations to *TRIO*, which result in premature stops and predicted nonsense mediated decay, are associated with neurodevelopmental disorders (82,102). Multiple studies have investigated how knock-down of Trio impacts cell signaling and morphology (see Chapter 1), but there has yet to be a study investigating a true loss of *TRIO*, excised from the genome. To excise Trio, a mouse model was utilized that harbors two loxP sites in introns flanking the first GEF1 domain(25) (141). Introduction of Cre recombinase and subsequent recombination results in a premature stop preceding the first GEF domain of *TRIO* (Fig. 3.1, *A*). Primary embryonic fibroblasts were harvested from the *TRIO*$^{fl/fl}$ mice and immortalized for future studies.

TABLE 3.1 CANDIDATE PROTEIN ACTIVATORS OF TRIO GEF1

	Protein class	Known effect on Trio/Trio based signaling	Known interaction with Trio	Reference
Neuroligin1	adhesion	Effects of D1368V in Trio9s on synaptogenesis dampened with inhibition of Neuroligin	Co-IP's with Trio9; Co-IP reduced by 50% with N1080I mutation	Tian 2021
ICAM1	adhesion	ICAM1 clustering increases amount of Trio pulled down by nucleotide free Rac1 and RhoG	Pulling down Myc-Trio FL or Myc-Trio-GEF1 also pulls down ICAM1 when both expressed in cells.	Van rijssel 2012
VE-Cadherin	adhesion	VE-cadherin recruits Trio to adherens junctions to induce activation of Rac1	GST SR5-6 interact with VE-cadherin peptide AA726-765 (purified proteins)	Timmerman 2015
Kidins220	adaptor	Overexpression of Kidins220 1-402 increases active Rac1 in cells	GST-Sec14, GST-SR1-4, and GST-SR5-9 all bind His-Kidins220 1-402 (purified proteins)	Neubrand 2010
ADAM23	adhesion	Loss of Trio correlates with lower expression levels of ADAM23	GST-ADAM23 can pull down Trio9s from cell lysate	Katrancha 2019
L1CAM	adhesion	Loss of Trio correlates with lower expression levels of L1CAM	Unable to confirm direct via pulldown from cell lysate	Katrancha 2019

TRIO$^{fl/fl}$ fibroblasts were transfected with GFP-P2A-Cre and allowed 5 days for recombination and full protein loss to occur. Cells were fixed and stained for GFP and Trio DH2, and DH2 fluorescence was quantified to determine the level of Trio knockout. Trio protein levels decreased by 30% upon transient transfection of Cre (Fig. 3.1, *B*), suggesting that the Trio fibroblast model could be a tractable model system for studying the impacts of global loss of Trio in cells (82).

3.4 Loss of Trio in fibroblasts changes cell morphology

Fibroblasts are an excellent system to investigate cell morphology and related signaling pathways. Many of these pathways are very well characterized. Therefore, we can get information from simple cell morphological changes about what major pathways may be impacted by events such as *TRIO* loss. This may also give insight into what the major functions of Trio, or major catalytic activities, are: for instance, specific cell morphology changes are associated with increased Rac1 or RhoA activity. Finally, it provides a tractable system to understand the effects of other protein interactors on Trio signaling.

Figure 3.1

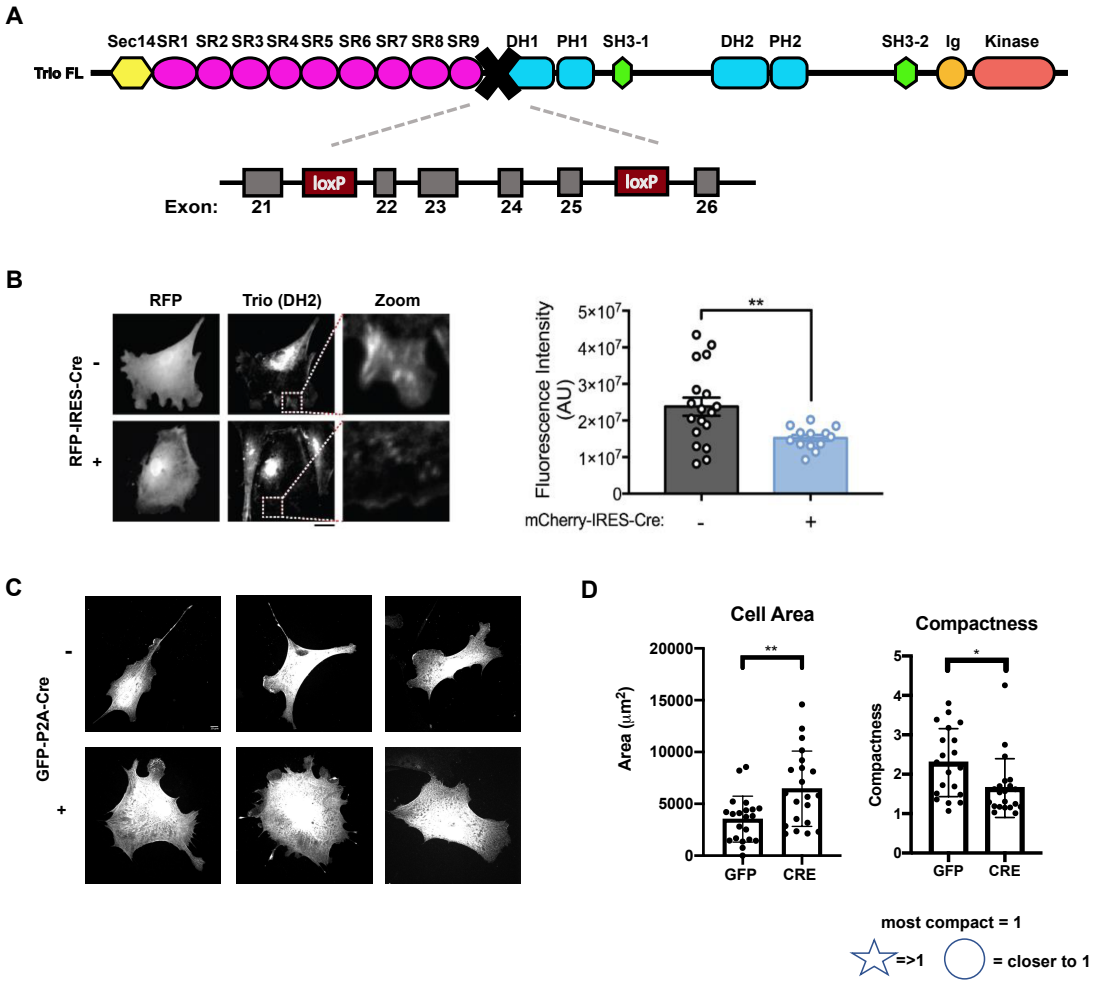

Fig. 3.1 Loss of TRIO impacts cells shape. Figure adapted from Katrancha et al., 2019

(A) Schematic of *TRIO*$^{fl/fl}$: loxP sites were inserted into introns flanking the first GEF domain of Trio (141). (B) Transient transfection of RFP-IRES-Cre into *TRIO*$^{fl/fl}$ fibroblasts results in a (Figure legend continued on next page)

(Figure legend 3.1 continued) loss of Trio protein. Trio protein was visualized using immunofluorescence against Trio DH2, and the fluorescence intensity was quantified. Originally published in Katrancha et al., 2019. (C) *TRIO*$^{fl/fl}$ cells transfected with GFP-P2A-Cre have altered cell morphology. Cell morphology was visualized using immunofluorescence against GFP, and cell area and compactness were quantified. Cells lacking Trio have an increased cell area and are more compact.

To understand how loss of Trio impacts cell morphology, I transfected GFP-P2A-Cre into *TRIO*$^{fl/fl}$ fibroblasts. Cells were plated on fibronectin-coated plates and allowed to spread before fixing and staining to visualize GFP (the presence of Cre), actin (phalloidin), and focal adhesions (vinculin/talin). General aspects of cell morphology were quantified. Cells expressing Cre had an overall larger cell area (Fig. 3.1, *C* and *D*). However, they also exhibited fewer long protrusions and were more compact – shaped more like circles than stars (Fig. 3.1, *D*). Additionally, these cells appeared to have enhanced stress fibers, though this was not quantified (Fig. 3.2, *A*). The effects of loss of Trio on cell morphology were especially interesting, considering that they mimicked that of Trio GEF1 overexpression (Figure 2.6). However, since Trio has two GEF activities, it is unclear what activity may be responsible for the observed changes in morphology. Rescue experiments using full-length Trio with each catalytic-dead variant will be critical in understanding this phenomenon.

Finally, to investigate cell adhesion pathways, I stained for vinculin and measured the distribution of focal adhesions. Focal adhesions are distributed about a cell differently depending on their maturity and their function in the cell (142). If a cell adhesion pathway were disrupted, we might expect the overall distribution of focal adhesions to change. However, no change in the distribution of focal adhesions was observed (Fig. 3.2, *B*). Total number of focal adhesions per condition was not analyzed, but would be useful to investigate in the future as well.

Based on these preliminary results, it appeared that loss of Trio impacted general facets of cell morphology. However, these studies were severely limited in their scope due to the very low transfection efficiency of fibroblasts. This motivated me to generate a stable cell line of *TRIO*$^{fl/fl}$ cells expressing GFP-Cre.

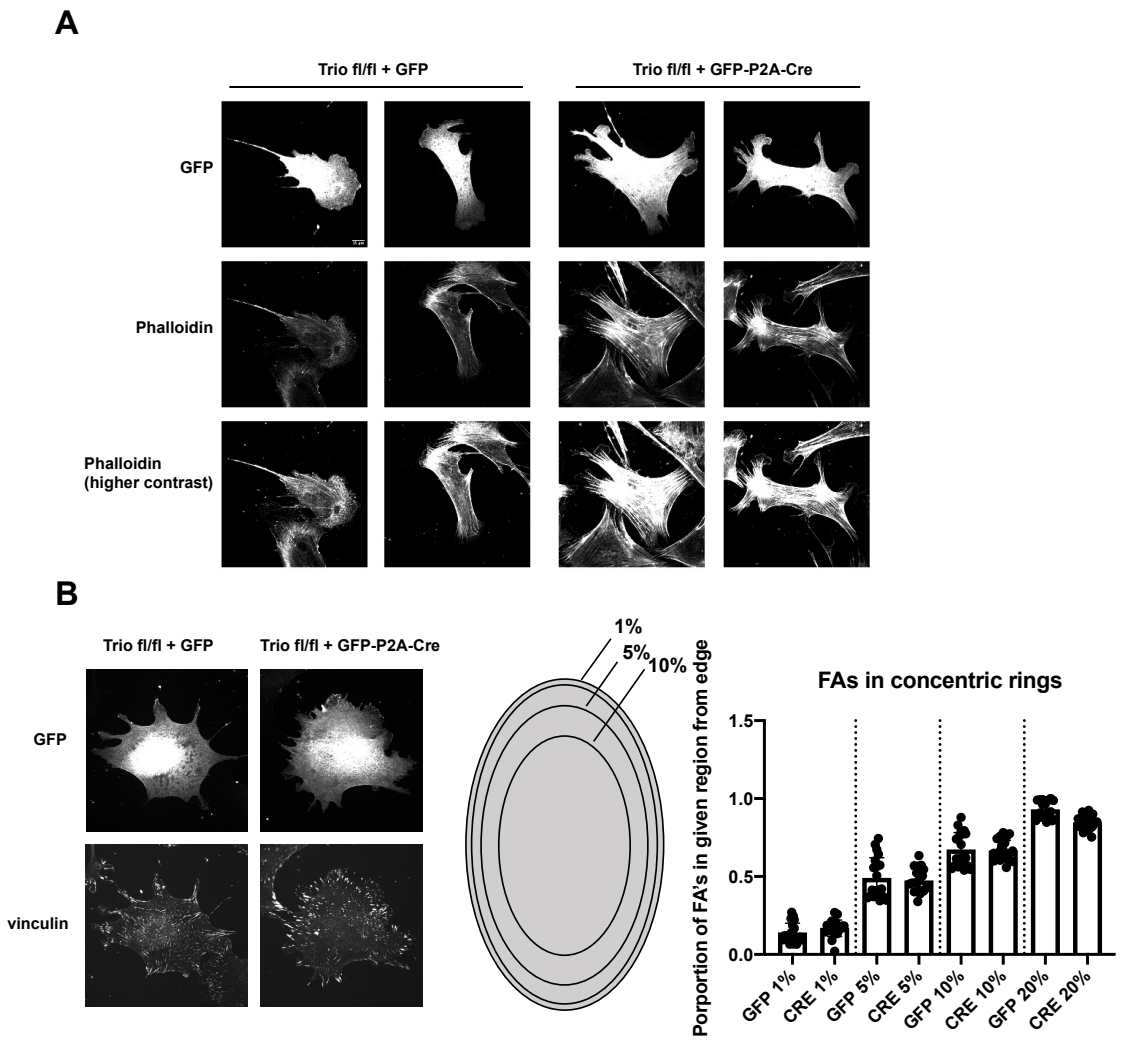

Fig. 3.2 Loss of Trio enhances stress fibers but has no effect on focal adhesion distribution.

(A) *TRIO*$^{fl/fl}$ cells transfected with GFP-P2A-Cre cells displayed enhanced abundance of stress fibers, visualized with fluorescent phalloidin. (B) *TRIO*$^{fl/fl}$ cells transfected with GFP-P2A-Cre displayed no change in focal adhesion (FA) organization. Focal adhesions (Figure legend continued on next page)

(Figure legend 3.2 continued) were visualized using immunofluorescent staining against vinculin. To determine the distribution of FAs, concentric cell outlines from the cell edge inward were drawn, scaled based on cell size. The quantity of focal adhesions relative to the total population was quantified, and showed no change between GFP and GFP-P2A-Cre transfected cells.

3.5 Generation of stable lines of Trio knockout cells

I sought to generate stable Trio knockout cell lines (Trio KO) by stable expression of GFP-Cre in *TRIO*$^{fl/fl}$ fibroblasts. I infected cells with a GFP-Cre retrovirus and selected the infected cells by puromycin resistance. Western blot confirmed loss of Trio FL in this cell population, and genotyping confirmed recombination at the loxP sites in Trio (Fig. 3.3, *A* and *B*). The cells appeared to have altered morphology compared to their parental line, especially at confluency: Trio KO cells packed more tightly and were less elongated than their parental line (Fig. 3.3, *C*). However, this cell line was generated using a polyclonal parental cell population. As a result, it was ultimately difficult to discern whether the infection had isolated one abnormal clonal population of cells, or if the effects we saw were actually due to Trio loss.

I subsequently isolated multiple monoclonal lines of the *TRIO*$^{fl/fl}$ parental cell population and infected these cells with the same GFP -Cre retrovirus. Attempts to validate this knockout gave unclear results, and have since been put on hold. The ambiguity of these results highlights obstacles in elucidating Trio function in a cellular context that must be considered for future studies. A big barrier to generating these cell lines is the lack of quality antibodies towards endogenous Trio. First, there are low levels of endogenous Trio in fibroblasts. Second, the antibodies we have towards Trio are polyclonal and affinity-purified, and as such,

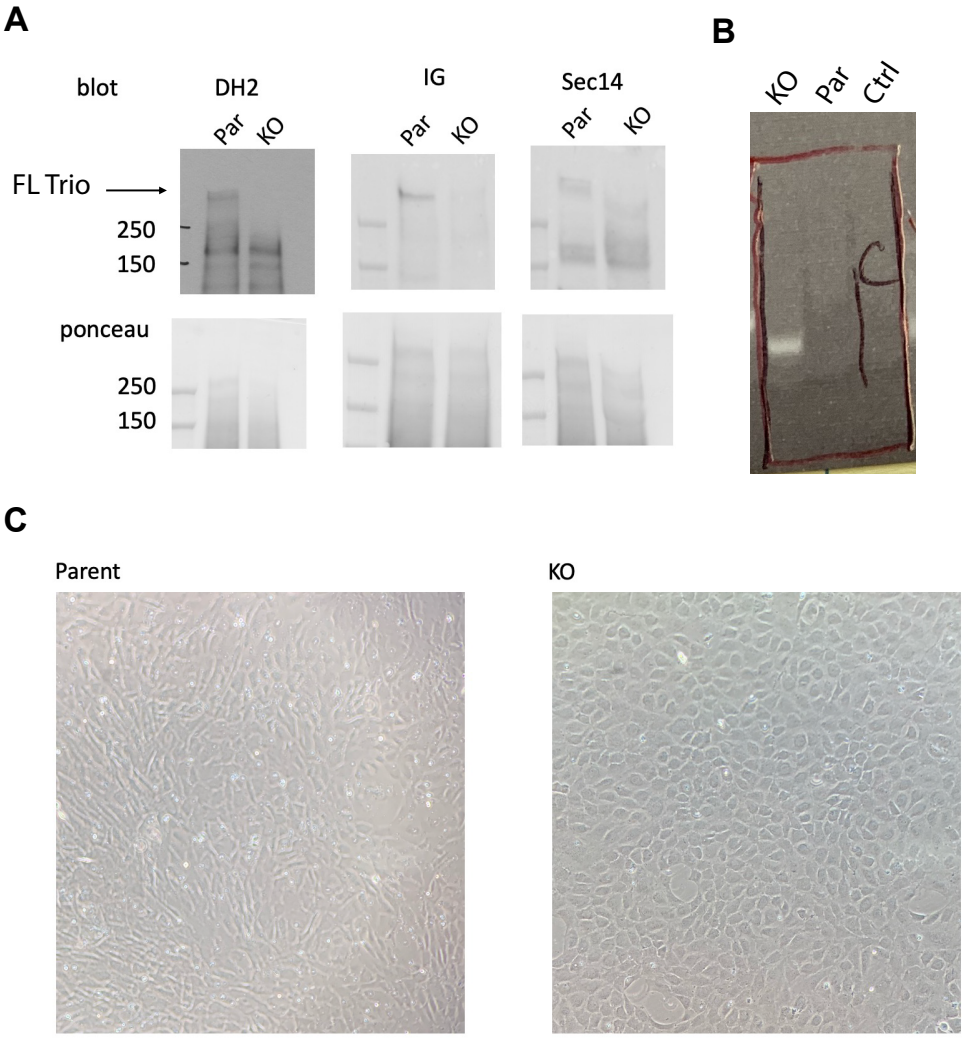

Fig. 3.3 Stable expression of GFP-P2A-Cre reduces Trio protein levels and alters cell packing morphology.

(A) *TRIO*$^{fl/fl}$ cells stably expressing GFP- Cre (KO) were analyzed for total protein levels using western blotting. Trio DH2, IG, and Sec14 antibodies were used to verify loss of Trio protein. (Figure legend continued on next page)

(Figure legend 3.3 continued) Full length Trio was almost completely eliminated in KO cells. (B) Recombination was verified in Trio KO cells using genotyping, demonstrated by the appearance of a band in the KO lane but not in the parental line. (C) Confluent KO cells exhibit tighter packing than the parental *TRIO*$^{fl/fl}$ line.

are relatively non-specific. Another obstacle to consider is that these antibodies may also recognize Kalirin protein fragments. Therefore, attempts to use western blot to determine total loss of protein levels almost always resulted in mixed results and unclear conclusions. I would argue that for this cell line to be successfully developed, these antibodies need to be better purified (perhaps against Kalirin protein fragments), further validated, or redesigned completely.

3.6 Trio interacts with ADAM23 cytoplasmic tail

Amanda and Tony purified GST fusions of the intracellular tails of ADAM23 (AA814-832) and L1CAM (AA1144-1257) (GST-ADAM23$_{tail}$ and GST-L1CAM$_{tail}$) (Fig. 3.4, *A* and *B*).

I first sought to investigate whether several candidate proteins identified via mass spectrometry directly interacted with Trio. I linked GST-ADAM23$_{tail}$ and GST-L1CAM$_{tail}$ to aminolink beads and incubated them with HEK293 lysate overexpressing Trio9s. Bound Trio9s was visualized by blotting for the Trio DH2 domain. GST-ADAM23$_{tail}$ was able to pull down protein at the size of Trio9s, whereas L1CAM$_{tail}$ was not, suggesting the ADAM23 cytoplasmic tail may interact with Trio9s (Fig. 3.4, *C*). It is still unclear which Trio9s domain interacts with ADAM23$_{tail}$, and if this interaction is direct. Amanda is following up on these studies to investigate ADAM22 binding, identify the regions of Trio involved in binding, and investigate pathways involving the upstream protein Lgi1.

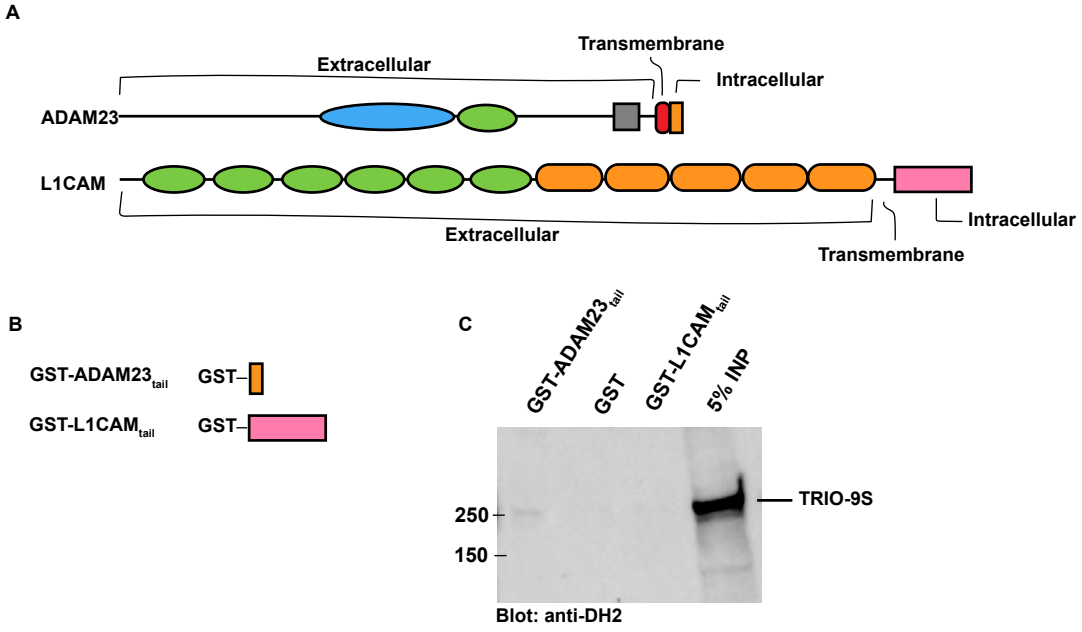

Fig. 3.4 Trio9s interacts with ADAM23.

(A) Schematic of full-length ADAM23 and L1CAM, with extracellular, transmembrane, and intracellular regions labeled. (B) Schematic of proteins purified and used in this study: the intracellular tails of ADAM23 and L1CAM. (C) Cell lysates overexpressing Trio-9s were incubated with GST fusion proteins linked to aminolink beads. Bound Trio-9s was visualized by blotting against Trio DH2. GST-ADAM23$_{tail}$ pulled down Trio9s, whereas GST or GST-L1CAM$_{tail}$ did not.

3.7 Generation of proteins to assay Trio GEF1 activation

As mentioned previously, several proteins are top candidate interactors due to previous work demonstrating their impact on Trio GEF1 activity in cells. However, it is unclear whether these proteins directly interact with Trio, and if they impact GEF1 activity via directly relieving autoinhibitory constraint or regulating GEF1 activity in a spatiotemporal manner. I therefore began generating DNA constructs for NLGN1, ICAM1, VE-Cadherin, and Kidins220 to test if these proteins have an effect on Trio GEF1 activity. Specifically, we are interested in whether these proteins can relieve the autoinhibition by the spectrin repeats in the context of SR6-GEF1. Ellen Corcoran and Anthony Koleske are currently continuing to generate these constructs to purify recombinant protein, and these studies will be ongoing.

3.8 Methods

$TRIO^{fl/fl}$ cell line generation, transfection, and infection

$TRIO^{fl/fl}$ fibroblasts were cultured and immortalized as described in (82). Clonal lines were developed by serial dilution of the *$TRIO^{fl/fl}$* fibroblasts to isolate single cells in conditioned medium and individual clones were expanded.

Lipofectamine was used to transfect *$TRIO^{fl/fl}$* cells with 0.5μg of GFP or GFP-P2A-Cre. Transfected cells were allowed to grow for 5 days to ensure loss of Trio. GFP-Cre retrovirus was generated using Bosc23 cells and was collected to infect *$TRIO^{fl/fl}$* cells. Infected cells were selected using 1μg/mL puromycin until control/ uninfected cells died.

Cell morphology analysis

Cell morphology was analyzed using immunofluorescence as described in Chapter 2.

Focal adhesions were semiautomatically identified with CellProfiler (138) using vinculin as a marker, and their distribution was determined based on their distance from the cell edge and quantified using a custom MATLAB script.

Western blotting and genotyping

Infected or transfected cells were lysed in lysis buffer (2% SDS, 5% glycerol, 250mM Tris pH 6.8) and western blotting was performed on lysate using 1:1000 Trio DH2, Kinase, Sec14, or SR56 primary antibodies and 1:4000 goat anti rabbit HRP. Blots were imaged using a Chemidoc (Bio-Rad).

For genotyping, infected cells were lysed in new gitshier buffer plus proteinase k (64mM Tris pH 8.8, 15.8mM $(NH_4)_2SO_4$, 6.2mM $MgCl_2$, 0.48% Triton X-100, 0.14mM BME, 0.35mg/mL proteinase K) and genotyped to verify recombination.

Tail binding pulldowns

HEK293 cells were transfected with HA-Trio9s using PEI, collected 24 hours post transfection, and lysed in coIP buffer (1% NP-40, 25mM HEPES pH 7.25, 5% Glycerol, 1mM EDTA, 100mM NaCl). GST-ADAM23$_{tail}$, GST-L1CAM$_{tail}$, and GST were purified from bacterial cells as described in Chapter 2. Proteins were dialyzed into PBS and linked to aminolink beads at a final concentration of 1mg/mL. Lysate

was diluted to 1mg/mL in coIP buffer and incubated with GST-bound beads for 30 minutes at 4°C (7.5μL beads per 500μL lysate) to minimize non-specific binding. 500μL precleared lysate was then incubated with 7.5μL beads for 2 hours at 4°C. Beads were washed quickly five times, and any Trio9s bound to beads was visualized via western blot.

Chapter 4

Future directions: a roadmap

4.1 Overview

In this chapter I discuss the most promising avenues for future projects related to regulation of GEF1 activity in Trio. These experiments are the cumulative result of numerous hours' worth of discussions among Ellen, Tony, and me. They range from the 'low-hanging fruit' questions that are immediately born out of the findings described in this dissertation, to the more ambitious questions that have puzzled the field for years.

4.2 Resolving finer structural details of SR6-GEF1

Our discovery that SR6-9 interacts with GEF1 has led us to ask several more specific questions. First, do the SRs inhibit GEF1 activity via sterically blocking access to Rac1, or via an allosteric mechanism? There are a few discrepancies between the AlphaFold model and the crosslinking data – what does the interaction interface between SR6-9 and GEF1 actually look like? Do all of the NDD-associated variants disrupt this SR6-9:GEF1 interaction, or do some act via a different mechanism? How do mutations to SR6 decrease GEF1 activity? Finally, are there structural subtleties that could provide information on why we only see a 2-fold decrease in the SR6-GEF1:Rac1 binding affinity, but a 10-fold decrease in catalytic efficiency? All of these questions require structural approaches to be resolved. I think that small angle x-ray scattering (SAXs), size exclusion chromatography, chemical crosslinking, and cryo-electron microscopy (cryo-EM) will provide great sources of information to address these questions.

We hypothesize that the interaction between SR6-9 and GEF1 results in a fairly globular protein structure, but that disease-associated mutations that hypothetically disrupt this interaction may elongate the overall protein. SAXs and SEC are both great approaches to this. Experiments using SEC to estimate the Stokes radius of the proteins are straightforward and unlikely to fail based on the monodisperse nature of all of our SR6-GEF1 variants; I highlight the major barriers to SAXs experiments below.

I attempted pilot experiments performing SAXs of wild-type SR6-GEF1 in collaboration with Kimmie Vish. To do these, I developed a purification scheme to generate highly purified product: following Ni-NTA affinity chromatography, I subjected the protein to anion exchange using a MonoQ column followed by size exclusion chromatography on a Superdex S200 Increase column. This yielded extremely pure protein. However, SAXs requires a significant amount of product at a moderate concentration (up to 2.5mg/mL). This purification scheme yielded sub-optimal amounts of protein, and the remaining protein was resistant to concentration in a minimal SAXs buffer (150mM KCl, 20mM HEPES pH 7.25, 1% glycerol; precipitates > 1mg/mL upon spin concentration). Careful optimization of the final concentrating steps in a SAXs-appropriate buffer will be likely to facilitate more successful SAXs experiments. From there, performing SAXs on mutants vs. WT SR6-GEF1 can provide insight into large-scale conformational changes that occur due to mutation. If our hypothesis is correct, we would expect to see more elongated structures in the SR6-GEF1 variants.

Chemical crosslinking may also provide fine details about intramolecular interactions that are disrupted due to disease associated mutations, and thus critical for autoinhibition. I performed chemical crosslinking experiments, identical to those described in Chapter 2, with three token mutants (SR6-GEF1$_{E883D}$, SR6-GEF1$_{R1078Q}$, and SR6-GEF1$_{D1368V}$) and am currently awaiting results.

Finally, solving a structure of SR6-GEF1 would be most illuminating in the search for structural details related to the SR6-9:GEF1 interaction interface and how mutations impact protein structure. Due to limitations in protein yield, cryo-EM is the optimal approach. We already have a method to generate high-purity protein, so one merely needs to engage a cryo-EM expert to help optimize grid conditions and collect and analyze data.

4.3 Activation pathways of Trio

After resolving the mechanism of autoinhibition of Trio GEF1 by the spectrin repeats, we were immediately curious how this autoinhibition might be released in cells. Based on the literature, there are several ‘candidate’ activating proteins that may release this autoinhibition, which I detail in Chapter 3. In this section, I describe an experimental framework for testing these ‘candidate’ activating proteins and detail an approach to identify new potential activating proteins that have not yet been identified in the literature.

The experiment for testing our existing ‘candidate’ activating proteins is simple: generate each protein and add it to a GEF assay with SR6-GEF1 and see if the

activity increases. Then one can dissect a mechanism of activation by determining binding affinity, stoichiometry, and interface between SR6-9 and the activating protein. We can then validate all of these details in vitro and in cells.

Experiments to identify new candidate activators not previously described in the literature are a little less straightforward. However, to start, we might hypothesize that a candidate activating protein utilizes interactions with the SRs to facilitate the autoinhibition release. Therefore, proteins that bind to SR6-9 would be great candidates for GEF1 regulation. I attempted pilot experiments to identify potential SR interactors: I tethered GST-SR6-9 to glutathione beads, incubated the beads with brain lysate, and analyzed bound proteins via SDS-PAGE. My results were ambiguous, and it was clear that non-specific binding needed to be mitigated before this experiment could yield any clear results. I also used GST-SR6-9 protein purified from bacteria, which we now believe is less soluble and pure than SR6-9 purified from insect cells. Using higher quality protein tethered to the beads may reduce nonspecific binding. Ideally, this experiment would resolve major bands that could be later identified via mass spectrometry. One would then purify the SR6-9 interacting protein and test its ability to activate SR6-GEF1 catalytic activity in vitro, then proceeding with the same set of experiments outlined in the previous paragraph.

An appealing expansion of this SR6-9:brain lysate pulldown experiment would be to tether SR6-9 disease-associated variants to beads and see if any interactions between WT and variant pulldowns differ. One could look for differences in major

bands on a pulldown gel visually, or perform a more thorough investigation using an approach like comparative mass spectrometry.

It is possible that the SR6-9:brain lysate pulldowns identify SR-interacting proteins that don't end up activating SR6-GEF1. These results could still be interesting and lend insight into aspects of GEF1 regulation other than release of autoinhibition. For instance, Rac1 activation is highly localized in a cell (143); perhaps a protein that binds SR6-9 positions Trio in an appropriate location of the cell for Rac1 activation. Any investigation of major Trio binding partners has will help create a fuller picture of Trio GEF regulation in a cellular context.

4.4. How are the two Trio GEF activities coordinated?

A longstanding question in the field is how the two GEF domains in Trio, which target opposing GTPases, are coordinated. Very little biochemistry has been performed to answer this question; this is not totally surprising, since (1) many larger fragments of Trio are difficult to purify and solubilize and (2) there isn't a very straightforward experiment to do to dissect these activities. However, the recent AlphaFold model of *Drosophila* trio (AF-Q7KVD1-F1 (126)) makes this question very enticing: not only do the SRs cradle the GEF1 domain, as shown in Fig. 2.4, but they also cradle the GEF2 domain (while there may not be as many possible interactions, the two GEF domains are placed adjacent to one another in space). This makes the idea of long-range intramolecular regulation (like between the SRs and GEF2 domain) particularly appealing and could explain how the multiple GEF activities are coordinated.

The simplest question to answer first is which GEF dominates, or has higher activity, when both are present. Previous work has shown that GEF2 has a four-times lower exchange rate for RhoA than GEF1 does for RhoG when tested as individual domains (22). However, a detailed analysis of the activities of these domains when they are both in the context of the same protein has never been done. Due to our extensive work purifying and solubilizing Trio fragments, I believe that we are well positioned to generate protein fragments that contain both GEF1 and GEF2. We also have a robust GEF assay to measure GEF activity that has been shown to measure the activities of both GEF1 and GEF2 (125), and a clever experiment could easily resolve some of these questions.

Conclusions

In this thesis I describe a novel mode of regulation of Trio GEF1 activity by the adjacent SRs. I discuss initial work to understand this regulation in a cellular context, and highlight the best avenues for future work. Beyond just illuminating a mechanism of regulation, this work has incredible potential for future translational work. *TRIO* mutations are associated with multiple neurodevelopmental disorders, and understanding how these mutations directly impact Trio function will guide the development of therapeutics.

References

1. Bircher, J. E., and Koleske, A. J. (2021) Trio family proteins as regulators of cell migration and morphogenesis in development and disease - mechanisms and cellular contexts. *J. Cell Sci* **134**
2. Bircher, J. E., Corcoran, E. E., Lam, T. T., Trnka, M. J., and Koleske, A. J. (2022 (submitted)) The Trio spectrin repeats inhibit its guanine nucleotide exchange factor activity for Rac1. *The Journal of biological chemistry*
3. Debant, A., Serra-Pages, C., Seipel, K., O'Brien, S., Tang, M., Park, S. H., and Streuli, M. (1996) The multidomain protein Trio binds the LAR transmembrane tyrosine phosphatase, contains a protein kinase domain, and has separate rac-specific and rho-specific guanine nucleotide exchange factor domains. *Proceedings of the National Academy of Sciences of the United States of America* **93**, 5466-5471
4. Alam, M. R., Caldwell, B. D., Johnson, R. C., Darlington, D. N., Mains, R. E., and Eipper, B. A. (1996) Novel Proteins that Interact with the COOH-terminal Cytosolic Routing Determinants of an Integral Membrane Peptide-processing Enzyme. *The Journal of biological chemistry* **271**, 28636
5. Steven, R., Kubiseski, T. J., Zheng, H., Kulkarni, S., Mancillas, J., Ruiz Morales, A., Hogue, C. W., Pawson, T., and Culotti, J. (1998) UNC-73 activates the Rac GTPase and is required for cell and growth cone migrations in C. elegans. *Cell* **92**, 785-795
6. Awasaki, T., Saito, M., Sone, M., Suzuki, E., Sakai, R., Ito, K., and Hama, C. (2000) The Drosophila trio plays an essential role in patterning of axons by regulating their directional extension. *Neuron* **26**, 119-131
7. McPherson, C. E., Eipper, B. A., and Mains, R. E. (2002) Genomic organization and differential expression of Kalirin isoforms. *Gene* **284**, 41-51
8. McPherson, C. E., Eipper, B. A., and Mains, R. E. (2005) Multiple novel isoforms of Trio are expressed in the developing rat brain. *Gene* **347**, 125-135
9. Miller, M. B., Yan, Y., Eipper, B. A., and Mains, R. E. (2013) Neuronal Rho GEFs in synaptic physiology and behavior. *The Neuroscientist : a review journal bringing neurobiology, neurology and psychiatry* **19**, 255-273
10. Alam, M. R., Johnson, R. C., Darlington, D. N., Hand, T. A., Mains, R. E., and Eipper, B. A. (1997) Kalirin, a cytosolic protein with spectrin-like and GDP/GTP exchange factor-like domains that interacts with peptidylglycine alpha-amidating monooxygenase, an integral membrane peptide-processing enzyme. *The Journal of biological chemistry* **272**, 12667-12675
11. Wu, J. H., Fanaroff, A. C., Sharma, K. C., Smith, L. S., Brian, L., Eipper, B. A., Mains, R. E., Freedman, N. J., and Zhang, L. (2013) Kalirin promotes neointimal hyperplasia by activating Rac in smooth muscle cells. *Arteriosclerosis, thrombosis, and vascular biology* **33**, 702-708
12. Ma, X. M., Huang, J. P., Eipper, B. A., and Mains, R. E. (2005) Expression of Trio, a member of the Dbl family of Rho GEFs in the developing rat brain. *The Journal of comparative neurology* **482**, 333-348

13. Ma, X. M., Johnson, R. C., Mains, R. E., and Eipper, B. A. (2001) Expression of kalirin, a neuronal GDP/GTP exchange factor of the trio family, in the central nervous system of the adult rat. *The Journal of comparative neurology* **429**, 388-402
14. Jaffe, A. B., and Hall, A. (2005) Rho GTPases: Biochemistry and Biology. *Annu Rev Cell Dev. Biol* **21**, 247-269
15. Penzes, P., Johnson, R. C., Alam, M. R., Kambampati, V., Mains, R. E., and Eipper, B. A. (2000) An isoform of kalirin, a brain-specific GDP/GTP exchange factor, is enriched in the postsynaptic density fraction. *The Journal of biological chemistry* **275**, 6395-6403
16. Wu, Y.-C., Cheng, T.-W., Lee, M.-C., and Weng, N.-Y. (2002) Distinct Rac Activation Pathways Control *Caenorhabditis elegans* Cell Migration and Axon Outgrowth. *Dev. Biol* **250**, 145-155
17. Kubiseski, T. J., Culotti, J., and Pawson, T. (2003) Functional Analysis of the *Caenorhabditis elegans* UNC-73B PH Domain Demonstrates a Role in Activation of the Rac GTPase In Vitro and Axon Guidance In Vivo. *Mol Cell Biol* **19**, 6823-6835
18. Blangy, A., Vignal, E., Schmidt, S., Debant, A., Gauthier-Rouviere, C., and Fort, P. (2000) TrioGEF1 controls Rac- and Cdc42-dependent cell structures through the direct activation of rhoG. *Journal of cell science* **113 (Pt 4)**, 729-739
19. Skowronek, K. R., Guo, F., Zheng, Y., and Nassar, N. (2004) The C-terminal basic tail of RhoG assists the guanine nucleotide exchange factor trio in binding to phospholipids. *The Journal of biological chemistry* **279**, 37895-37907
20. Chhatriwala, M. K., Betts, L., Worthylake, D. K., and Sondek, J. (2007) The DH and PH domains of Trio coordinately engage Rho GTPases for their efficient activation. *J Mol Biol* **368**, 1307-1320
21. Penzes, P., Johnson, R. C., Kambampati, V., Mains, R. E., and Eipper, B. A. (2001) Distinct roles for the two Rho GDP/GTP exchange factor domains of kalirin in regulation of neurite growth and neuronal morphology. *The Journal of neuroscience : the official journal of the Society for Neuroscience* **21**, 8426-8434
22. Bellanger, J. M., Estrach, S., Schmidt, S., Briancon-Marjollet, A., Zugasti, O., Fromont, S., and Debant, A. (2003) Different regulation of the Trio Dbl-Homology domains by their associated PH domains. *Biology of the cell / under the auspices of the European Cell Biology Organization* **95**, 625-634
23. Peurois, F., Veyron, S., Ferrandez, Y., Ladid, I., Benabdi, S., Zeghouf, M., Peyroche, G., and Cherfils, J. (2017) Characterization of the activation of small GTPases by their GEFs on membranes using artificial membrane tethering. *Biochem J* **474**, 1259-1272
24. Yan, Y., Eipper, B. A., and Mains, R. E. (2016) Kalirin is required for BDNF-TrkB stimulated neurite outgrowth and branching. *Neuropharmacology* **107**, 227-238
25. Peng, Y. J., He, W. Q., Tang, J., Tao, T., Chen, C., Gao, Y. Q., Zhang, W. C., He, X. Y., Dai, Y. Y., Zhu, M. S., and al., e. (2010) Trio is a key guanine nucleotide exchange factor coordinating regulation of the migration and morphogenesis of granule

cells in the developing cerebellum. *The Journal of biological chemistry* **285**, 24834-24844
26. Backer, S., Lokmane, L., Landragin, C., Deck, M., Garel, S., and Bloch-Gallego, E. (2018) Trio GEF mediates RhoA activation downstream of Slit2 and coordinates telencephalic wiring. *Development* **145**
27. Valdivia, A., Goicoechea, S. M., Awadia, S., Zinn, A., and Garcia-Mata, R. (2017) Regulation of circular dorsal ruffles, macropinocytosis, and cell migration by RhoG and its exchange factor, Trio. *Molecular biology of the cell* **28**, 1768-1781
28. van Leeuwen, F. N., Kain, H. E. T., van der Kammen, R. A., Michiels, F., Kranenburg, O. W., and Collard, J. G. (1997) The Guanine Nucleotide Exchange Factor Tiam1 Affects Neuronal Morphology; Opposing Roles for the Small GTPases Rac and Rho. *The Journal of cell biology* **139**, 797-807
29. Sander, E. E., ten Klooster, J. P., van Delft, S., van der Kammen, R. A., and Collard, J. G. (1999) Rac downregulates Rho activity: reciprocal balance between both GTPases determines cellular morphology and migratory behavior. *The Journal of cell biology* **147**, 1009-1022
30. Gauthier-Rouviere, C., Vignal, E., Meriane, M., Roux, P., Montcourier, P., and Fort, P. (1998) RhoG GTPase Controls a Pathway That Independently Activates Rac1 and Cdc42Hs. *Molecular biology of the cell* **9**, 1379-1394
31. Katoh, H., and Negishi, M. (2003) RhoG activates Rac1 by direct interaction with the Dock180-binding protein Elmo. *Nature* **424**, 461-464
32. van Rijssel, J., and van Buul, J. D. (2012) The many faces of the guanine-nucleotide exchange factor trio. *Cell Adh Migr* **6**, 482-487
33. Liu, X., Wang, H., Eberstadt, M., Schnuchel, A., Olejniczak, E., Meadows, R. P., Schkeryantz, J. M., Janowick, D. A., Harlan, J. E., Fesik, S. W., and al., e. (1999) NMR Structure and Mutagenesis of the N-Terminal Dbl Homology Domain of the Nucleotide Exchange Factor Trio. *Cell* **95**, 269-277
34. Bandekar, S. J., Arang, N., Tully, E. S., Tang, B. A., Barton, B. L., Li, S., Gutkind, J. S., and Tesmer, J. J. G. (2019) Structure of the C-terminal guanine nucleotide exchange factor module of Trio in an autoinhibited conformation reveals its oncogenic potential. *Sci Signal* **12**
35. Chen, S.-Y., Huang, P.-H., and Cheng, H.-J. (2011) Disrupted-in-Schizophrenia 1-mediated axon guidance involves TRIO-RAC-PAK small GTPase pathway signaling. *PNAS* **108**, 5861-5866
36. Schiller, M. R., Chakrabarti, K., King, G. F., Schiller, N. I., Eipper, B. A., and Maciejewski, M. W. (2006) Regulation of RhoGEF activity by intramolecular and intermolecular SH3 domain interactions. *The Journal of biological chemistry* **281**, 18774-18786
37. Schiller, M. R., Ferraro, F., Wang, Y., Ma, X. M., McPherson, C. E., Sobota, J. A., Schiller, N. I., Mains, R. E., and Eipper, B. A. (2008) Autonomous functions for the Sec14p/spectrin-repeat region of Kalirin. *Experimental cell research* **314**, 2674-2691
38. Kawai, T., Sanjo, H., and Akiran, S. (1999) Duet is a novel serine/threonine kinase with Dbl-Homology (DH) and Pleckstrin-Homology (PH) domains. *Gene* **227**

39. Kiraly, D. D., Stone, K. L., Colangelo, C. M., Abbott, T., Wang, Y., Mains, R. E., and Eipper, B. A. (2011) Identification of kalirin-7 as a potential post-synaptic density signaling hub. *Journal of proteome research* **10**, 2828-2841
40. Sonoshita, M., Itatani, Y., Kakizaki, F., Sakimura, K., Terashima, T., Katsuyama, Y., Sakai, Y., and Taketo, M. M. (2015) Promotion of colorectal cancer invasion and metastasis through activation of NOTCH-DAB1-ABL-RHOGEF protein TRIO. *Cancer Discov* **5**, 198-211
41. Ma, X. M., Miller, M. B., Vishwanatha, K. S., Gross, M. J., Wang, Y., Abbott, T., Lam, T. T., Mains, R. E., and Eipper, B. A. (2014) Nonenzymatic domains of Kalirin7 contribute to spine morphogenesis through interactions with phosphoinositides and Abl. *Molecular biology of the cell* **25**, 1458-1471
42. Forsthoefel, D. J., Liebl, E. C., Kolodziej, P. A., and Seeger, M. A. (2005) The Abelson tyrosine kinase, the Trio GEF and Enabled interact with the Netrin receptor Frazzled in Drosophila. *Dev* **132**, 1983-1994
43. Miller, M. B., Yan, Y., Machida, K., Kiraly, D. D., Levy, A. D., Wu, Y. I., Lam, T. T., Abbott, T., Koleske, A. J., Eipper, B. A., and Mains, R. E. (2017) Brain Region and Isoform-Specific Phosphorylation Alters Kalirin SH2 Domain Interaction Sites and Calpain Sensitivity. *ACS chemical neuroscience* **8**, 1554-1569
44. Xin, X., Wang, Y., Ma, X. M., Rompolas, P., Keutmann, H. T., Mains, R. E., and Eipper, B. A. (2008) Regulation of Kalirin by Cdk5. *Journal of cell science* **121**, 2601-2611
45. DeGeer, J., Boudeau, J., Schmidt, S., Bedford, F., Lamarche-Vane, N., and Debant, A. (2013) Tyrosine phosphorylation of the Rho guanine nucleotide exchange factor Trio regulates netrin-1/DCC-mediated cortical axon outgrowth. *Mol Cell Biol* **33**, 739-751
46. Xie, Z., Srivastava, D. P., Photowala, H., Kai, L., Cahill, M. E., M., W. K., Shum, C. Y., Surmeier, D. J., and Penzes, P. (2007) Kalirin-7 Controls Activity-Dependent Structural and Functional Plasticity of Dendritic Spines. *Neuron* **56**, 640-656
47. Xin, X., Ferraro, F., Back, N., Eipper, B. A., and Mains, R. E. (2004) Cdk5 and Trio modulate endocrine cell exocytosis. *Journal of cell science* **117**, 4739-4748
48. Yan, Y., Eipper, B. A., and Mains, R. E. (2014) Kalirin-9 and Kalirin-12 Play Essential Roles in Dendritic Outgrowth and Branching. *Cerebral cortex*
49. Bellanger, J. M., Astier, C., Sardet, C., Ohta, Y., Stossel, T. P., and Debant, A. (2000) The Rac1- and RhoG-specific GEF domain of Trio targets filamin to remodel cytoskeletal actin. *Nat. Cell. Biol.* **2**, 888-892
50. Seipel, K., O'Brien, S. P., Iannotti, E., Medley, Q. G., and Streuli, M. (2000) Tara, a novel F-actin binding protein, associates with the Trio guanine nucleotide exchange factor and regulates actin cytoskeletal organization. *Journal of cell science* **114**, 389-399
51. Koo, T. H., Eipper, B. A., and Donaldson, J. G. (2007) Arf6 recruits the Rac GEF Kalirin to the plasma membrane facilitating Rac activation. *BMC cell biology* **8**, 29
52. Tao, T., Sun, J., Peng, Y., Li, Y., Wang, P., Chen, X., Zhao, W., Zheng, Y. Y., Wei, L., Zhu, M. S., and al., e. (2019) Golgi-resident TRIO regulates membrane trafficking during neurite outgrowth. *The Journal of biological chemistry* **294**, 10954-10968

53. Kroon, J., Heemskerk, N., Kalsbeek, M. J. T., de Waard, V., van Rijssel, J., and van Buul, J. D. (2017) Flow-induced endothelial cell alignment requires the RhoGEF Trio as a scaffold protein to polarize active Rac1 distribution. *Molecular biology of the cell* **28**, 1745-1753
54. Medley, Q. G., Buchbinder, E. G., Tachibana, K., Ngo, H., Serra-Pages, C., and Streuli, M. (2003) Signaling between focal adhesion kinase and trio. *The Journal of biological chemistry* **278**, 13265-13270
55. Sun, Y. J., Nishikawa, K., Yuda, H., Wang, Y. L., Osaka, H., Fukazawa, N., Naito, A., Kudo, Y., Wada, K., and Aoki, S. (2006) Solo/Trio8, a membrane-associated short isoform of Trio, modulates endosome dynamics and neurite elongation. *Mol Cell Biol* **26**, 6923-6935
56. Chenette, E. J., and Der, C. J. (2011) 5-Lipid Modification of Ras Superfamily GTPases: Not Just Membrane Glue. in *The Enzymes* (Tamanoi, F., Hrycyna, C. A., and Bergo, M. O. eds.), Academic Press. pp 59-95
57. Miller, M. B., Vishwanatha, K. S., Mains, R. E., and Eipper, B. A. (2015) An N-terminal Amphipathic Helix Binds Phosphoinositides and Enhances Kalirin Sec14 Domain-mediated Membrane Interactions. *The Journal of biological chemistry* **290**, 13541-13555
58. van Rijssel, J., Hoogenboezem, M., Wester, L., Hordijk, P. L., and Van Buul, J. D. (2012) The N-terminal DH-PH domain of Trio induces cell spreading and migration by regulating lamellipodia dynamics in a Rac1-dependent fashion. *PloS one* **7**, e29912
59. Ridley, A. (2001) Rho GTPases and cell migration. *Journal of cell science* **114**, 2713-2722
60. Forrester, W. C., and Garriga, G. (1997) Genes necessary for C. elegans cell and growth cone migrations. *Dev* **124**
61. Lundquist, E. A., Reddien, P. W., Hartwieg, E., Horvitz, H. R., and Bargmann, C. i. (2001) Three *C. elegans* Rac proteins and several alternative Rac regulators control axon guidance, cell migration, and apoptotic cell phagocytosis. *Dev* **128**, 4475-4488
62. Spencer, A. G., Orita, S., Malone, C. J., and Han, M. (2001) A RHO GTPase-mediated pathway is required during P cell migration in *Caenorhabditis elegans*. *PNAS* **98**, 13132-13137
63. Vanderzalm, P. J., Pandey, A., Hurwitz, M. E., Bloom, L., Horvitz, H. R., and Garriga, G. (2009) C. elegans CARMIL negatively regulates UNC-73/Trio function during neuronal development. *Development* **136**, 1201-1210
64. Zipkin, I. D., Kindt, R. M., and Kenyon, C. J. (1997) Role of a New Rho Family Member in Cell Migration and Axon Guidance in C. elegans. *Cell* **90**, 883-894
65. Son, K., Smith, T. C., and Luna, E. J. (2015) Supervillin Binds the Rac/Rho-GEF Trio and Increases Trio-Mediated Rac1 Activation. *Cytoskeleton* **72**, 47-64
66. van Haren, J., Boudeau, J., Schmidt, S., Basu, S., Liu, Z., Lammers, D., Demmers, J., Benhari, J., Grosveld, F., Galjart, N., and al., e. (2014) Dynamic microtubules catalyze formation of navigator-TRIO complexes to regulate neurite extension. *Current biology : CB* **24**, 1778-1785

67. Yano, T., Yamazaki, Y., Adachi, M., Okawa, K., Fort, P., Uji, M., Tsukita, S., and Tsukita, S. (2011) Tara up-regulates E-cadherin transcription by binding to the Trio RhoGEF and inhibiting Rac signaling. *The Journal of cell biology* **193**, 319-332
68. Seipel, K., Medley, Q. G., Kedersha, N. L., Zhang, X. A., O'Brien, S. P., Serra-Pages, C., Hemler, M. E., and Streuli, M. (1999) Trio amino-terminal guanine nucleotide exchange factor domain expression promotes actin cytoskeleton reorganization, cell migration, and anchorage-independent cell growth. *J. Cell Sci* **112**, 1825-1834
69. Blangy, A., Bouquier, N., Gauthier-Rouviere, C., Schmidt, S., Debant, A., Leonetti, J. P., and Fort, P. (2006) Identification of TRIO-GEFD1 chemical inhibitors using the yeast exchange assay. *Biology of the cell / under the auspices of the European Cell Biology Organization* **98**, 511-522
70. Ferraro, F., Ma, X. M., Sobota, J. A., Eipper, B. A., and Mains, R. E. (2007) Kalirin/Trio Rho guanine nucleotide exchange factors regulate a novel step in secretory granule maturation. *Molecular biology of the cell* **18**, 4813-4825
71. Bouquier, N., Vignal, E., Charrasse, S., Weill, M., Schmidt, S., Leonetti, J. P., Blangy, A., and Fort, P. (2009) A cell active chemical GEF inhibitor selectively targets the Trio/RhoG/Rac1 signaling pathway. *Chem Biol* **16**, 657-666
72. Bellanger, J. M., Lazaro, J. B., Diriong, S., Fernandez, A., Lamb, N., and Debant, A. (1998) The two guanine nucleotide exchange factor domains of Trio link the Rac1 and the RhoA pathways in vivo. *Oncogene* **16**, 147-152
73. Schiller, M. R., Blangy, A., Huang, J., Mains, R. E., and Eipper, B. A. (2005) Induction of lamellipodia by Kalirin does not require its guanine nucleotide exchange factor activity. *Experimental cell research* **307**, 402-417
74. Liang, Y., Niederstrasser, H., Edwards, M., Jackson, C. E., and Cooper, J. A. (2009) Distinct Roles for CARMIL Isoforms in Cell Migration. *Molecular biology of the cell* **20**
75. Walck-Shannon, E., Reiner, D., and Hardin, J. (2015) Polarized Rac-dependent protrusions drive epithelial intercalation in the embryone epidermis of *C. elegans*. *Development* **142**, 3549-3560
76. Bateman, J., Shu, H., and Van Vactor, D. (2000) The Guanine Nucleotide Exchange Factor Trio Mediates Axonal Development in the *Drosophila* Embryo. *Neuron* **26**, 93-106
77. Newsome, T. P., Schmidt, S., Dietzl, G., Keleman, K., Asling, B., Debant, A., and Dickson, B. J. (2000) Trio combines with dock to regulate Pak activity during photoreceptor axon pathfinding in Drosophila. *Cell* **101**, 283-294
78. Briancon-Marjollet, A., Ghogha, A., Nawabi, H., Triki, I., Auziol, C., Fromont, S., Piche, C., Enslen, H., Chebli, K., Lamarche-Vane, N., and al., e. (2008) Trio mediates netrin-1-induced Rac1 activation in axon outgrowth and guidance. *Mol Cell Biol* **28**, 2314-2323
79. DeGeer, J., Kaplan, A., Mattar, P., Morabito, M., Stochaj, U., Kennedy, T. E., Debant, A., Cayouette, M., Fournier, A. E., and Lamarche-Vane, N. (2015) Hsc70 chaperone activity underlies Trio GEF function in axon growth and guidance induced by netrin-1. *The Journal of cell biology* **210**, 817-832

80. Watari-Goshima, N., Ogura, K.-i., Wolf, F. W., Goshima, Y., and Garriga, G. (2007) *C. elegans* VAB-8 and UNC-73 regulate the SAX-3 receptor to direct cell and growth-cone migrations. *Nat Neuro* **10**, 169-176
81. Li, J., Pu, P., and Le, W. (2013) The SAX-3 Receptor Stimulates Axon Outgrowth and the Signal Sequence and Transmembrane Domain Are Critical for SAX-3 Membrane Localization in the PDE Neuron of *C. elegans*. *PloS one* **8**
82. Katrancha, S. M., Shaw, J. E., Zhao, A. Y., Myers, S. A., Cocco, A. R., Jeng, A. T., Zhu, M., Pittenger, C., Greer, C. A., Koleske, A. J., and al., e. (2019) Trio Haploinsufficiency Causes Neurodevelopmental Disease-Associated Deficits. *Cell Rep* **26**, 2805-2817 e2809
83. May, V., Schiller, M. R., Eipper, B. A., and Mains, R. E. (2002) Kalirin Dbl-homology guanine nucleotide exchange factor 1 domain initiates new axon outgrowths via RhoG-mediated mechanisms. *The Journal of neuroscience : the official journal of the Society for Neuroscience* **22**, 6980-6990
84. Ma, X. M., Kiraly, D. D., Gaier, E. D., Wang, Y., Kim, E. J., Levine, E. S., Eipper, B. A., and Mains, R. E. (2008) Kalirin-7 is required for synaptic structure and function. *The Journal of neuroscience : the official journal of the Society for Neuroscience* **28**, 12368-12382
85. Penzes, P., Beeser, A., Chernoff, J., Schiller, M. R., Eipper, B. A., Mains, R. E., and Huganir, R. L. (2003) Rapid induction of dendritic spine morphogenesis by trans-synaptic ephrinB-EphB receptor activation of the Rho-GEF kalirin. *Neuron* **37**, 263-274
86. Paskus, J., Tian, C., Fingleton, E., Shen, C., Chen, X., Li, Y., Myers, S. A., Badger II, J. D., Bemben, M. A., Herring, B. E., and Roche, K. W. (2019) Synaptic Kalirin-7 and Trio Interactomes Reveal a GEF Protein-Dependent Neuroligin-1 Mechanism of Action. *Cell Rep* **29**, 2944-2952
87. Alexander, M., Selman, G., Seetharaman, A., Chan, K. K. M., D'Souza, S. A., Byrne, A. B., and Roy, P. J. (2010) MADD-2, a Homolog of the Opitz Syndrome Protein MID1, Regulates Guidance to the Midline through UNC-40 in *Caenorhabditis elegans*. *Dev. Cell* **18**, 961-972
88. Timmerman, I., Heemskerk, N., Kroon, J., Schaefer, A., van Rijssel, J., Hoogenboezem, M., van Unen, J., Goedhart, J., Gadella, T. W. J., van Buul, J. D., and al., e. (2015) A local VE-cadherin and Trio-based signaling complex stabilizes endothelial junctions through Rac1. *J. Cell Sci* **128**, 3041-3054
89. Polacheck, W. J., Kutys, M. L., Yang, J., Eyckmans, J., Wu, Y., Vasavada, H., Hirschi, K. K., and Chen, C. S. (2017) A non-canonical Notch complex regulats adherens junctions and vascular barrier function. *Nature* **552**, 258-262
90. Kruse, K., Lee, Q. S., Sun, Y. J., Klomp, J., Yang, X., Huang, F., Sun, M. Y., Zhao, S., Hong, Z., Vogel, S., Shin, J.-., Leckband, D. E., Tai, L. M., Malik, A. B., and Komarova, Y. A. (2018) N-cadherin signaling via Trio assembles adherens junctions to restrict endothelial permeability. *The Journal of cell biology* **281**, 299-316

91. Vestweber, D. (2008) VE-Cadherin The Major Endothelial Adhesion Molecule Controlling Cellular Junctions and Blood Vessel Formation. *Arteriosclerosis, thrombosis, and vascular biology* **28**, 223-232
92. Henrique, D., and Schweisguth, F. (2019) Mechanisms of Notch signaling: a simple logic deployed in time and space. *Development* **146**
93. van Rijssel, J., Kroon, J., Hoogenboezem, M., van Alphen, F. P., de Jong, R. J., Kostadinova, E., Geerts, D., Hordijk, P. L., and van Buul, J. D. (2012) The Rho-guanine nucleotide exchange factor Trio controls leukocyte transendothelial migration by promoting docking structure formation. *Molecular biology of the cell* **23**, 2831-2844
94. Van Rijssel, J., Timmerman, I., Van Alphen, F. P., Hoogenboezem, M., Korchynskyi, O., Geerts, D., Geissler, J., Reedquist, K. A., Niessen, H. W., and Van Buul, J. D. (2013) The Rho-GEF Trio regulates a novel pro-inflammatory pathway through the transcription factor Ets2. *Biol Open* **2**, 569-579
95. Charrasse, S., Comunale, F., Fortier, M., Portales-Casamar, E., Debant, A., and Gauthier-Rouviere, C. (2007) M-Cadherin Activates Rac1 GTPase through the Rho-GEF Trio during Myoblast Fusion. *Molecular biology of the cell* **18**, 1734-1743
96. Mains, R. E., Alam, M. R., Johnson, R. C., Darlington, D. N., Back, N., Hand, T. A., and Eipper, B. A. (1999) Kalirin, a multifunctional PAM COOH-terminal domain interactor protein, affects cytoskeletal organization and ACTH secretion from AtT-20 cells. *The Journal of biological chemistry* **274**, 2929-2937
97. Hu, S., Pawson, T., and Steven, R. (2011) UNC-73/Trio RhoGEF-2 Activity Modulates *Caenorhabditis elegans* Motility Through Changes in Neurotransmitter Signaling Upstream of the GSA-1/GalphaS Pathway. *Genetics* **189**, 137-151
98. Herring, B. E., and Nicoll, R. A. (2016) Kalirin and Trio proteins serve critical roles in excitatory synaptic transmission and LTP. *Proceedings of the National Academy of Sciences of the United States of America* **113**, 2264-2269
99. Xin, X., Rabiner, C. A., Mains, R. E., and Eipper, B. A. (2009) Kalirin12 interacts with dynamin. *BMC neuroscience* **10**, 61
100. Lin, Y. C., and Koleske, A. J. (2010) Mechanisms of synapse and dendrite maintenance and their disruption in psychiatric and neurodegenerative disorders. *Annual review of neuroscience* **33**, 349-378
101. Sadybekov, A., Tian, C., Arnesano, C., Katritch, V., and Herring, B. E. (2017) An autism spectrum disorder-related de novo mutation hotspot discovered in the GEF1 domain of Trio. *Nat Commun* **8**, 601
102. Singh, T., Poterba, T., Curtis, D., Akil, H., Al Eissa, M., Barchas, J. D., Bass, N., Bigdeli, T. B., Breen, G., Daly, M. J., and al., e. (2020) Exome sequencing identifies rare coding variants in 10 genes which confer substantial risk for schizophrenia. *medRxiv*, 2020.2009.2018.20192815
103. Hill, J. J., Hashimoto, T., and Lewis, D. A. (2006) Molecular mechanisms contributing to dendritic spine alterations in the prefrontal cortex of subjects with schizophrenia. *Mol Psychiatry* **11**, 557-566

104. Kushima, I., Nakamura, Y., Aleksic, B., Ikeda, M., Ito, Y., Shiino, T., Okochi, T., Fukuo, Y., Ujike, H., Suzuki, M., Inada, T., Hashimoto, R., Takeda, M., Kaibuchi, K., Iwata, N., and Ozaki, N. (2010) Resequencing and Association Analysis of the KALRN and EPHB1 Genes and Their Contribution to Schizophrenia Suscepitibility. *Schizophr. Bull.*
105. Youn, H., Jeoung, M., Koo, Y., Ji, H., Markesbery, W. R., Ji, I., and H., J. T. (2007) Kalirin is Under-Expressed in Alzheimer's Disease Hippocampus. *J. Alzheimers Dis.* **11**
106. Wang, L., Hauser, E. R., Shah, S., Pericak-Vance, M. A., Haynes, C., Crosslin, D., Harris, M., Nelson, S., Hale, A. B., Vance, J. M., and al., e. (2007) Peakwide Mapping on Chromosome 3q13 Identifies Kalirin Gene as a Novel Candidate Gene for Coronary Artery Disease. *Am J Hum Genet* **80**, 650-663
107. Krug, T., Manso, H., Gouveia, L., Sobral, J., Xavier, J. M., Albergaria, I., Gaspar, G., Correia, M., Viana-Baptista, M., Oliveria, S. A., and al., e. (2010) Kalirin: a novel genetic risk factor for ischemic stroke. *Human Genetics* **127**, 513-523
108. Rudock, M. E., Cox, A. J., Ziegler, J. T., Lehtinen, A. B., Connelly, J. J., Freedman, B. I., Carr, J. J., Lengefeld, C. D., Hauser, E. R., Horne, B. D., and Bowden, D. W. (2011) Cigarette smoking status has a modifying effect on the association between polymorphisms in KALRN and measure of cardiovascular risk in the diabetes heart study. *Genes and Genomics* **33**
109. Ikram, M. A., Seshadri, S., Bis, J. C., Fornage, M., DeStefano, A. L., Aulchenko, Y. S., Debette, S., Lumley, T., Folsom, A. R., Wolf, P. A., and al., e. (2009) Genomewide Association Studies of Stroke. *N Engl J Med.* **360**, 1718-1728
110. Zheng, M., Simon, R., Mirlacher, M., Maurer, R., Gasser, T., Forster, T., Diener, P. A., Mihatsch, M. J., Sauter, G., and Schraml, P. (2004) *TRIO* Amplification and Abundant mRNA Expression is Associated with Invasive Tumor Growth and Rapid Tumor Cell Proliferation in Urinary Bladder Cancer. *Am J Pahol.* **165**, 63-69
111. Baldwin, C., Garnis, C., Zhang, L., Rosin, M. P., and Lam, W. L. (2005) Multiple Microalterations Detected at High Frequency in Oral Cancer. *Cancer Res.* **65**, 7561-7567
112. Lane, J., Martin, T. A., Mansel, R. E., and Jiang, W. G. (2008) The expression and prognostic value of the guanine nucleotide exchange factors (GEFs) Trio, Vav1 and TIAM-1 in human breast cancer. *Int Semin Surg Oncol* **5**, 23
113. Chattopadhyay, I., Singh, A., Phukan, R., Purkayastha, J., Kataki, A., Mahanta, J., Saxena, S., and Kapur, S. (2010) Genome-wide analysis of chromosomal alterations in patients with esophageal squamous cell carcinoma exposed to tobacco and betel quid from high-rish area in India. *Mutat Res.* **696**, 130-138
114. Coe, B. P., Henderson, L.-J., Garnis, C., Tsao, M.-S., Gazdar, A. F., Minna, J., Lam, S., MacAulay, C., and Lam, W. L. (2005) High-Resolution Chromosome Arm 5p Array CGH Analysis of Small Cell Lung Carcinoma Cell Lines. *Genes Chromosomes Cancer* **42**, 308-313
115. Salhia, B., Tran, N. L., Chan, A., Wolf, A., Nakada, M., Rutka, F., Ennis, M., McDonough, W. S., Berens, M. E., Rutka, J. T., and al., e. (2008) The Guanine

Nucleotide Exchange Factors Trio, Ect2, and Vav3 Mediate the Invasive Behavior of Glioblastoma. *Am. J. Pathol.* **173**, 1828-1838
116. Wang, B., Fang, J., Qu, L., Cao, Z., Zhou, J., and Deng, B. (2015) Upregulated TRIO expression correlates with a malignant phenotype in human hepatocellular carcinoma. *Tumour Biol.* **36**, 6901-6908
117. Hou, C., Zhuang, Z., Deng, X., Xu, Y., Zhang, P., and Zhu, L. (2018) Knockdown of Trio by CRISPR/Cas9 suppresses migration and invasion of cervical cancer cells. *Oncol Rep* **39**, 795-801
118. Adamowicz, M., Radlwimmer, B., Riker, R. J., Mertens, D., Schwarzbach, M., Shchraml, P., Benner, A., Lichter, P., Mechtersheimer, G., and Joos, S. (2006) Frequent Amplifications and Abundant Expression of TRIO, NKD2, and IRX2 in Soft Tissue Sarcomas. *Genes Chromosomes Cancer* **45**, 829-838
119. Vaque, J. P., Dorsam, R. T., Feng, X., Iglesias-Bartolome, R., Forsthoefel, D. J., Chen, Q., Debant, A., Seeger, M. A., Ksander, B. R., Teramoto, H., and Gutkind, J. S. (2013) A Genome-wide RNAi Screen Reveals a Trio-Regulated Rho GTPase Circuitry Transducing Mitogenic Signals Initiated by G Protein-Coupled Receptors. *Mol Cell* **49**
120. Katrancha, S. M., Wu, Y., Zhu, M., Eipper, B. A., Koleske, A. J., and Mains, R. E. (2017) Neurodevelopmental disease-associated de novo mutations and rare sequence variants affect TRIO GDP/GTP exchange factor activity. *Hum Mol Genet* **26**, 4728-4740
121. Barbosa, S., Greville-Heygate, S., Bonnet, M., Godwin, A., Fagotto-Kaufmann, C., Kajava, A. V., laouteouet, D., mawby, R., Aung Wai, H., Baralle, D., and al., e. (2020) Opposite Modulation of RAC1 by Mutations in TRIO is Associated with Distinct, Domain-Specific Neurodevelopmental Disorders. *Am. J. Hum. Genet* **106**, 338-355
122. Pengelly, R. J., Greville-Heygate, S., Schmidt, S., Seaby, E. G., Jabalameli, M. R., Mehta, S. G., Parker, M. J., Goudie, D., Fagotto-Kaufmann, C., Baralle, D., and al., e. (2016) Mutations specific to the Rac-GEF domain of TRIO cause intellectual disability and microcephaly. *J. Med Genet* **53**, 735-742
123. Paskus, J., Herring, B. E., and Roche, K. W. (2020) Kalirin and Trio: RhoGEFs in Synaptic Transmission, Plasticity, and Complex Brain Disorders. *Trends in neurosciences* **43**, 505-518
124. Estrach, S., Schmidt, S., Diriong, S., Penna, A., Blangy, A., Fort, P., and Debant, A. (2002) The Human Rho-GEF trio and its target GTPase RhoG are involved in the NGF pathway, leading to neurite outgrowth. *Current biology : CB* **12**, 307-312
125. Blaise, A. M., Corcoran, E. E., Wattenberg, E., Zhang, Y.-L., and Koleske, A. J. (2021) In vitro fluorescence assay to measure GDP/GTP exchange of guanine nucleotide exchange factors of Rho family GTPases.
126. Jumper, J., Evans, R., Pritzel, A., Green, T., Figurnov, M., Ronneberger, O., Tunyasuvunakool, K., Bates, R., Žídek, A., Potapenko, A., Bridgland, A., Meyer, C., Kohl, S. A. A., Ballard, A. J., Cowie, A., Romera-Paredes, B., Nikolov, S., Jain, R., Adler, J., Back, T., Petersen, S., Reiman, D., Clancy, E., Zielinski, M., Steinegger, M., Pacholska, M., Berghammer, T., Bodenstein, S., Silver, D., Vinyals, O., Senior,

A. W., Kavukcuoglu, K., Kohli, P., and Hassabis, D. (2021) Highly accurate protein structure prediction with AlphaFold. *Nature* **596**, 583-589
127. Ward, J. J., McGuffin, L. J., Bryson, K., Buxton, B. F., and Jones, D. T. (2004) The DISOPRED server for the prediction of protein disorder. *Bioinformatics* **20**, 2138-2139
128. Hall, A. (1998) Rho GTPases and the actin cytoskeleton. *Science* **279**, 509-514
129. Debreceni, B., Gao, Y., Guo, F., Zhu, K., Jia, B., and Zheng, Y. (2004) Mechanisms of guanine nucleotide exchange and Rac-mediated signaling revealed by a dominant negative trio mutant. *The Journal of biological chemistry* **279**, 3777-3786
130. Xu, Z., Gakhar, L., Bain, F. E., Spies, M., and Fuentes, E. J. (2017) The Tiam1 guanine nucleotide exchange factor is auto-inhibited by its pleckstrin homology coiled-coil extension domain. *The Journal of biological chemistry* **292**, 17777-17793

131. Tian, C., Paskus, J. D., Fingleton, E., Roche, K. W., and Herring, B. E. (2021) Autism Spectrum Disorder/Intellectual Disability-Associated Mutations in Trio Disrupt Neuroligin 1-Mediated Synaptogenesis. *2021* **41**, 7768-7778
132. Terry-Lorenzo, R. T., Torres, V. I., Wagh, D., Galaz, J., Swanson, S. K., Florens, L., Washburn, M. P., Waites, C. L., Gundelfinger, E. D., Garner, C. C., and al., e. (2016) Trio, a Rho Family GEF, Interacts with the Presynaptic Active Zone Proteins Piccolo and Bassoon. *PloS one* **11**, e0167535
133. Neubrand, V. E., Thomas, C., Schmidt, S., Debant, A., and Schiavo, G. (2010) Kidins220/ARMS regulates Rac1-dependent neurite outgrowth by direct interaction with the RhoGEF Trio. *Journal of cell science* **123**, 2111-2123
134. Sanchez, N. A., Kallweit, L. M., Trnka, M. J., Clemmer, C. L., and Al-Sady, B. (2021) Heterodimerization of H3K9 histone methyltransferases G9a and GLP activates methyl reading and writing capabilities. *The Journal of biological chemistry* **297**
135. Schnirch, L., Nadler-Holly, M., Siao, S.-W., Frese, C. K., Viner, R., and Liu, F. (2020) Expanding the Depth and Sensitivity of Cross-Link Identification by Differential Ion Mobility Using High-Field Asymmetric Waveform Ion Mobility Spectrometry. *Anal Chem* **92**, 10495-10503
136. Trnka, M. J., Baker, P. R., Robinson, P. J. J., Burlingame, A. L., and Chalkley, R. J. (2014) Matching cross-linked peptide spectra: only as good as the worse identification. *Mol Cell Proteomics* **13**, 420-434
137. Lim, C., Berk, J. M., Blaise, A. M., Bircher, J. E., Koleske, M. H., and Xiong, Y. (2020) Crystal structure of a guanine nucleotide exchange factor encoded by the scrub typhus pathogen Orientia tsutsugamushi. *PNAS* **117**, 30380-30390
138. Mcquin, C., Goodman, A., Cherynyshev, V., Kamentsky, L., Cimini, B. A., Karhos, K. W., Doan, M., Ding, L., Rafelski, S. M., Thirstrup, D., Wiegraebe, W., Singh, S., Becker, T., Caicedo, J. C., and Carpenter, A. E. (2018) CellProfiler 3.0: Next-generation image processing for biology. *PLos Biol* **16**

139. Markus-Koch, A., Schmitt, O., Seemann, S., Lukas, J., Koczan, D., Ernst, M., Georg, F., Wree, A., Rolfs, A., and Luo, J. (2017) ADAM23 promotes neuronal differentiation of human neural progenitor cells. *CMBL* **22**
140. Samatov, T. R., Wicklein, D., and Tonevitsky, A. G. (2016) L1CAM: Cell adhesion and more. *Prog Histochem Cytochem* **51**
141. Zong, W., Liu, S., Wang, X., Zhang, J., Zhang, T., Liu, Z., Wang, D., Zhang, A., Zhu, M., and Gao, J. (2015) Trio gene is required for mouse learning ability. *Brain Res* **1608**, 82-90
142. Gallant, N. D., and Elineni, K. K. (2011) Regulation of Cell Adhesion Strength by Peripheral Focal Adhesion Distribution. *Biophys J* **101**, 2903-2911
143. Martin, K., Reiman, A., Fritz, R. D., Ryu, H., Jeon, N. L., and Pertz, O. (2016) Saptio-temporal co-ordination of RhoA, Rac1, and Cdc42 activation during prototypical edge protrusion and retraction dynamics. *Nat Sci Rep* **6**